

Supporting information

1,3-Dioxolane compounds (DOXs) as biobased reaction media

Massimo Melchiorre,^{a,b} Peter H. M. Budzelaar,^a Maria E. Cucciolito,^{a,c} Roberto Esposito,^{a,c} Emanuela Santagata,^a and Francesco Ruffo*,^{a,c}

^a Dipartimento di Scienze Chimiche, Università degli Studi di Napoli Federico II, Complesso Universitario di Monte S. Angelo, Via Cintia 21, 80126, Napoli, Italy.

^b ISusChem S.r.l., Piazza Carità 32, 80134 Napoli, Italy.

^c Consorzio Interuniversitario di Reattività Chimica e Catalisi (CIRCC), Via Celso Ulipiani 27, 70126, Bari, Italy.

Table of Contents

General.....	3
DOXs synthesis	3
5-methyl-1,3-dioxolan-4-one (LA-H,H).....	3
2,5-dimethyl-1,3-dioxolan-4-one (LA-H,Me).....	3
2,2,5-trimethyl-1,3-dioxolan-4-one (LA-Me,Me).....	3
5-phenyl-1,3-dioxolan-4-one (MA-H,H).....	3
5,5-dimethyl-1,3-dioxolan-4-one (iBu-H,H).....	3
2,2,5,5-tetramethyl-1,3-dioxolan-4-one (iBu-Me,Me).....	4
Table S1 DOXs solvents isolated yield. Boiling point at 1 atm estimated by nomograph.....	4
Fig. S1 ¹ H NMR (top) and ¹³ C NMR (bottom) spectra of LA-H,H.....	5
Fig. S2 ¹ H NMR (top) and ¹³ C NMR (bottom) spectra of LA-H,Me. Diastereomers ratio 70:30.....	6
Fig. S3 ¹ H NMR (top) and ¹³ C NMR (bottom) spectra of LA-Me,Me.....	7
Fig. S4 ¹ H NMR (top) and ¹³ C NMR (bottom) spectra of MA-H,H.....	8
Fig. S5 ¹ H NMR (top) and ¹³ C NMR (bottom) spectra of iBu-H,H.....	9
Fig. S6 ¹ H NMR (top) and ¹³ C NMR (bottom) spectra of iBu-Me,Me.....	10
Kamlet-Taft parameters determination.....	11
Fig. S7a Calibration line and ν_{\max} of dyes in each DOX.....	11
Fig. S7b Calibration line and ν_{\max} of dyes in iBu-Me,Me.....	12
Table S2 Absorption frequencies dyes in DOXs expressed in kK.....	12
Hansen and Teas parameters determination.....	12
Table S3 Hansen parameters for LA-H,H defined with Stefanis group contribution method.....	13
Table S4 Hansen parameters for LA-H,Me defined with Stefanis group contribution method.....	14
Table S5 Hansen parameters for LA-Me,Me defined with Stefanis group contribution method.....	14
Table S6 Hansen parameters for MA-H,H defined with Stefanis group contribution method.....	15
Table S7 Hansen parameters for iBu-H,H defined with Stefanis group contribution method.....	15
Table S8 Hansen parameters for iBu-Me,Me defined with Stefanis group contribution method.....	16
Fig. S8 3D Hansen space for fossil-based (black), green (green), and DOXs (red) solvents. LA-H,Me and iBu-Me,Me overlaps.....	17
Table S9. Distance in tridimensional Hansen space among commercial polar aprotic solvents and DOXs solvents. ACN, acetonitrile; DCM, dichloromethane; DMF, dimethylformamide; DMSO, dimethylsulphoxide; NMP, N-methyl pyrrolidone; THF, tetrahydrofuran; PC, propylene carbonate; DMI, dimethyl isosorbide; GVL, γ -valerolactone. Data with $R_a < 5$ are marked in bold.....	17
Table S10 Hansen parameters of common polymers used to calculate RED vs DOXs solvents.....	18
Table S11 Relative energy difference (RED) between common polymers and DOXs solvents. When RED < 1 the affinity between solvents and polymer is high. Data with RED < 1 are marked in bold.....	19
Fig. S9 Teas plot representation of fossil-based (black), green (green) and DOXs (red) solvents.....	20

Fig. S10 Thermal liquid range (mp and bp) at ambient pressure of DOXs and commercial polar aprotic solvents (green and fossil based). Melting point for LA-X,X are below -70 °C.....	21
Fig. S11 Flash points of DOXs and commercial polar aprotic solvents (green and fossil based).....	21
Fig. S12 Mizoroki-Heck coupling in LA-H,H. Traces 1 (0.5 h) and 2 (24 h) of Table 3 Entry 1.....	22
Fig. S13. Mizoroki-Heck coupling in LA-H,Me. Traces 1 (0.5 h) and 2 (24 h) of Table 3 Entry 2.....	22
Fig. S14 Mizoroki-Heck coupling in LA-Me,Me. Traces 1 (0.5 h) and 2 (24 h) of Table 3 Entry 3.....	23
Fig. S15 Mizoroki-Heck coupling in MA-H,H.Traces 1 (0.5 h) and 2 (24 h) of Table 3 Entry 4.....	23
Fig. S16 Mizoroki-Heck coupling in iBu-H,H. Traces 1 (0.5 h) and 2 (24 h) of Table 3 Entry 5.....	24
Fig. S17 Mizoroki-Heck coupling in iBu-Me,Me. Traces 1 (0.5 h) and 2 (24 h) of Table 3 Entry 6.....	24
Fig. S18. ¹ H NMR signal assignment of Mizoroki-Heck reaction mixture in LA-H,H.	25
Fig. S19. Relevant portion of ¹ H NMR of Menschutkin reaction in DMSO (left) and LA-H,H (right). Trace 1, 2, 3, 4, 5 represent crude reaction mixture at different time: 0.5 (bottom), 1, 2, 4, 24 (top) hours.	25
Fig. S20 ¹ H NMR of 1-butyl-3-methyl-imidazolium iodide isolated from LA-H,H.	26
Fig. S21 ¹ H NMR of LA-H,H (0.5mL) treated with different bases (0.07 mmol) at 100 °C for 24 h.....	26
Fig. S22. ¹ H NMR of LA-H,H (0.5 mL) treated with <i>p</i> -TsOH for 24 h at RT (trace 1) and 50 °C (trace 2). HMB added as standard.	27
Fig. S23 ¹ H NMR of LA-H,H (0.5 mL) treated with <i>p</i> -TsOH (0.07 mmol) for 24 h at 100 °C. HMB added as standard.....	27
Fig. S24 ¹ H NMR in DMSO-d6 of LA-H,H (0.5 mL) treated with concentrated HCl (5μL, 0.07 mmol) for 24 h at RT (trace 1); 0.5 mL of acetic acid/sodium acetate buffer solution (pH 4.7) after 24 h (trace 2) and after two weeks (trace 3).	28
Fig. S25 LA-H,H miscibility table. Also LA-H,Me and MA-H,H resulted immiscible with <i>n</i> -hexane, <i>n</i> -heptane and cyclohexane., LA-Me,Me, iBu-H,H and iBu-Me,Me resulted miscible with <i>n</i> -hexane.	29
Fig. S26. Relevant portion of ¹ H NMR of reaction mixture in presence of unreacted reagent (phenyl iodide) and product (methyl cinnamate). Yield is calculated by the following equation (13)	29
Table S12 Mutagenicity and carcinogenicity <i>in silico</i> results. Average result: mutagenic – average score > 0.5; non-mutagenic average score <0.5; n.a. - not applicable.	30

General

All reagents and solvents were purchased from Merck-Life Science and used without further purification. Nuclear magnetic resonance spectra were recorded with a Bruker Avance Ultrashield 400 spectrometer operating at a proton frequency of 400 MHz or a Varian Oxford 500 machine operating at a proton frequency of 500 MHz. The following abbreviations were used for describing NMR multiplicities: s, singlet; d, doublet; t, triplet; q, quartet; m, multiplet; dd, doublet of doublets. UV-Visible spectra were recorded with a Jasco V-700 spectrophotometer in the range of 700-200 nm. Flash points were estimated using T.E.S.T. software¹ Version 5.1.2 developed by Environmental Protection Agency (EPA), US. Boiling points at reduced pressure were determined during vacuum distillation. Melting points were determined using dry ice/acetone cold bath. Stability tests with bases and *p*-toluenesulfonic acid monohydrate (*p*-TsOH·H₂O) were performed treating 0.5 mL of LA-H,H with 0.7 mmol of the proper compound for 24 h at the selected temperature (RT, 50 °C and 100 °C). Stability towards aqueous acids was evaluated treating 0.5 mL of LA-H,H with 0.5 mL of buffer solution (pH 4.7 acetic acid/acetate) and with 5 µL of HCl 37 %wt, in both cases for 24 h at room temperature. Miscibility was tested by treating 100 µL of LA-H,H with an equal volume of the desired solvent. Solubility of LA-H,H in aliphatic solvents (*n*-hexane, cyclohexane and *n*-heptane) was determined by ¹H NMR from corresponding saturated solutions. For chiral solvents, the polarized-light rotation angle of the neat solvent was recorded with a Jasco P-1020 polarimeter, using a quartz cuvette (1 cm optical path length) at room temperature. Toxicity prediction was performed using three open-source software: VEGA² (mutagenicity - CAESAR, SARpy, ISS and KNN models), Toxtree³ (mutagenicity – ISS model; carcinogenicity and mutagenicity – ISS model) and T.E.S.T.¹ (mutagenicity – Consensus method).

DOXs synthesis

5-methyl-1,3-dioxolan-4-one (LA-H,H). For the synthesis of LA-H,H the procedure reported by Cairns et al.⁴ has been followed with some modifications. 45.0 g of DL-lactic acid (0.500 mol), 22.5 g of paraformaldehyde (0.750 mol), 125 mL of petroleum ether (bp: 40–60 °C), and 1.5 g of *p*-TsOH·H₂O (0.0075 mol) as a Brønsted acid catalyst were added in a 500 mL round-bottom flask equipped with a 25 mL Dean-Stark trap and Allihn condenser. The reaction mixture was refluxed under vigorous magnetic stirring for 24 h. Then the crude mixture was cooled in an ice bath and treated with 3.0 g of Na₂CO₃ (0.015 mol) for 30 min. The reaction crude was filtered, and the volatile solvent evaporated under reduced pressure. The product was isolated by vacuum distillation (8 mbar) at 36–38 °C. The enantiopure solvent was obtained starting from L-(+)-lactic acid using the same procedure. ¹H NMR (500 MHz, CDCl₃) δ 5.52 (s, 1H), 5.40 (s, 1H), 4.28 (q, *J* = 6.8 Hz, 1H), 1.49 (d, *J* = 6.8 Hz, 3H). ¹³C NMR (101 MHz, CDCl₃) δ 173.62, 93.93, 69.63, 15.82 (Fig. S1).

2,5-dimethyl-1,3-dioxolan-4-one (LA-H,Me). For the synthesis of LA-H,Me the procedure reported by Okada et al.⁵ has been followed with some modifications. 18.0 g of DL-lactic acid (0.200 mol), 13 mL of paraldehyde (0.100 mol), 260 mL of petroleum ether (bp: 60–80 °C) and 1.6 g of Amberlite® IR-120 (H⁺ form) as heterogeneous Brønsted acid catalyst were added in a 500 mL round-bottom flask equipped with a 25 mL Dean–Stark trap and Allihn condenser. The mixture was refluxed under magnetic stirring for 3 h. The crude mixture was cooled to room temperature and filtered to remove the catalyst. The volatile solvent was removed, and the product was isolated by vacuum distillation (22 mbar) at 54–56 °C. The product was obtained as cis-trans diastereomer mixture in a 70:30 ratio. Major stereoisomer: ¹H NMR (400 MHz, CDCl₃) δ 5.60 (q, *J* = 4.9 Hz, 1H), 4.32 (q, *J* = 6.7 Hz, 1H), 1.55 (d, *J* = 5.0 Hz, 3H), 1.52 (d, *J* = 7.0 Hz, 3H). ¹³C NMR (101 MHz, CDCl₃) δ 174.09, 101.64, 71.81, 20.41, 16.39. Minor stereoisomer: ¹H NMR (400 MHz, CDCl₃) δ 5.84 (q, *J* = 5.0 Hz, 1H), 4.50 (q, *J* = 7.0 Hz, 1H), 1.49 (d, *J* = 5 Hz, 3H), 1.44 (d, *J* = 7.0 Hz, 3H). ¹³C NMR (101 MHz, CDCl₃) δ 174.04, 102.11, 70.35, 20.82, 15.76. (Fig. S2).

2,2,5-trimethyl-1,3-dioxolan-4-one (LA-Me,Me). For the synthesis of LA-Me,Me the procedure reported by Miyagawa et al.⁶ has been followed with some modifications. 9.0 g of DL-lactic acid (0.10 mol), 60 mL of a solution 1:1 v/v acetone (0.40 mol) / petroleum ether (bp:40–60 °C), and 0.28 g of *p*-TsOH·H₂O (0.0015 mol) as a Brønsted acid catalyst were added in a 100 mL round-bottom flask equipped with a 25 mL Dean–Stark trap and Allihn condenser. The reaction mixture was refluxed for 24 h under magnetic stirring. After reaction time, the crude mixture was placed in an ice bath and treated with 0.32 g of Na₂CO₃ (0.003 mol) for 30 min. The reaction crude was filtered, and volatile solvent evaporated under reduced pressure. The product was isolated by vacuum distillation (9 mbar) at 42–44 °C. Enantiopure solvent was obtained starting from L-(+)-lactic acid using the same procedure. ¹H NMR (400 MHz, CDCl₃) δ 4.48 (q, *J* = 6.8 Hz, 1H), 1.61 (s, 3H), 1.54 (s, 3H), 1.48 (d, *J* = 6.8 Hz, 3H) ¹³C NMR (101 MHz, CDCl₃) δ 173.85, 110.34, 70.43, 27.43, 25.59, 17.38. (Fig. S3).

5-phenyl-1,3-dioxolan-4-one (MA-H,H). For the synthesis of MA-H,H the procedure reported by Xu et al.⁷ has been followed with some modifications. 15.0 g of DL-mandelic acid (0.100 mol), 5.0 g of paraformaldehyde (0.160 mol), 320 mL of cyclohexane and 2.0 g of *p*-TsOH·H₂O (0.010 mol) as a Brønsted acid catalyst were added in a 500 mL round-bottom flask equipped with a 25 mL Dean-Stark trap and Allihn condenser. The mixture was refluxed under vigorous magnetic stirring for 3 h. The crude mixture was washed with water, and the organic phase evaporated under reduced pressure. The product was isolated by vacuum distillation (120–125 °C) at 10–15 mbar. The enantiopure solvent was obtained starting from D-(−)-mandelic acid using the same procedure. ¹H NMR (500 MHz, CDCl₃) δ 7.50 – 7.36 (m, 5H), 5.70 (s, 1H), 5.63 (s, 1H), 5.24 (s, 1H). ¹³C NMR (101 MHz, CDCl₃) δ 171.28, 133.21, 129.14, 128.81 (2C), 126.43 (2C), 94.47, 74.39 (Fig. S4).

5,5-dimethyl-1,3-dioxolan-4-one (iBu-H,H). For the synthesis of iBu-H,H the procedure reported by Clive et al.⁸ has been followed with some modifications. 21.0 g of α-hydroxyisobutyric acid (0.200 mol), 9.0 g of paraformaldehyde (0.300 mol),

100 mL of petroleum ether (bp: 40–60 °C), and 9.0 g of *p*-TsOH·H₂O (0.003 mol) as a Brønsted acid catalyst were added in a 250 mL round-bottom flask equipped with a 25 mL Dean–Stark trap and Allihn condenser. The reaction was refluxed under vigorous magnetic stirring for 24 h. After the reaction time, the crude mixture was cooled in an ice bath and treated with 0.65 g of Na₂CO₃ (0.006 mol) for 30 min. The reaction crude was then filtered, and the volatile solvent evaporated under reduced pressure. The product was isolated by vacuum distillation (70 mbar) at 60–62 °C. ¹H NMR (500 MHz, CDCl₃) δ 5.44 (s, 2H), 1.45 (s, 6H). ¹³C NMR (101 MHz, CDCl₃) δ 175.37, 91.95, 75.21, 22.21 (2C) (Fig. S5).

2,2,5,5-tetramethyl-1,3-dioxolan-4-one (iBu-Me,Me). For the synthesis of iBu-Me,Me, the procedure reported by Watanabe et al.⁹ has been followed with some modifications. 10.4 g of α-hydroxyisobutyric acid (0.100 mol), 120 mL of a solution 1:1 v/v acetone (0.800 mol) and petroleum ether (bp:40–60 °C), and 2.0 g of *p*-TsOH·H₂O (0.010 mol) as a Brønsted acid catalyst were added in a 250 mL round-bottom flask equipped with a 25 mL Dean–Stark trap and Allihn condenser. The reaction mixture was refluxed for 48 h under magnetic stirring. The crude mixture was placed in an ice bath and treated with 3.2 g of Na₂CO₃ (0.03 mol) for 30 min. The reaction crude was filtered, and the volatile solvent evaporated under reduced pressure. The product was isolated by vacuum distillation (15 mbar) at 38–40 °C.

¹H NMR (500 MHz, CDCl₃) δ 1.57 (s, 6H), 1.48 (s, 6H). ¹³C NMR (101 MHz, CDCl₃) δ 176.00, 109.50, 77.58, 28.61 (2C), 26.52 (2C). (Fig. S6).

Table S1 DOXs solvents isolated yield. Boling point at 1 atm estimated by nomograph.

Solvents	Isolated yield [%]	Distillation pressure [mbar]	Distillation temperature [°C]	Boiling point normalized to 1 atm [°C]
LA-H,H	60	8	36-38	161-164
LA-H,Me	10	22	54-56	163-165
LA-Me,Me	50	9	42-44	166-169
MA-H,H	50	10-15	120-125	250-260
iBu-H,H	77	70	60-62	141-143
iBu -Me,Me	25	15	38-40	150-153

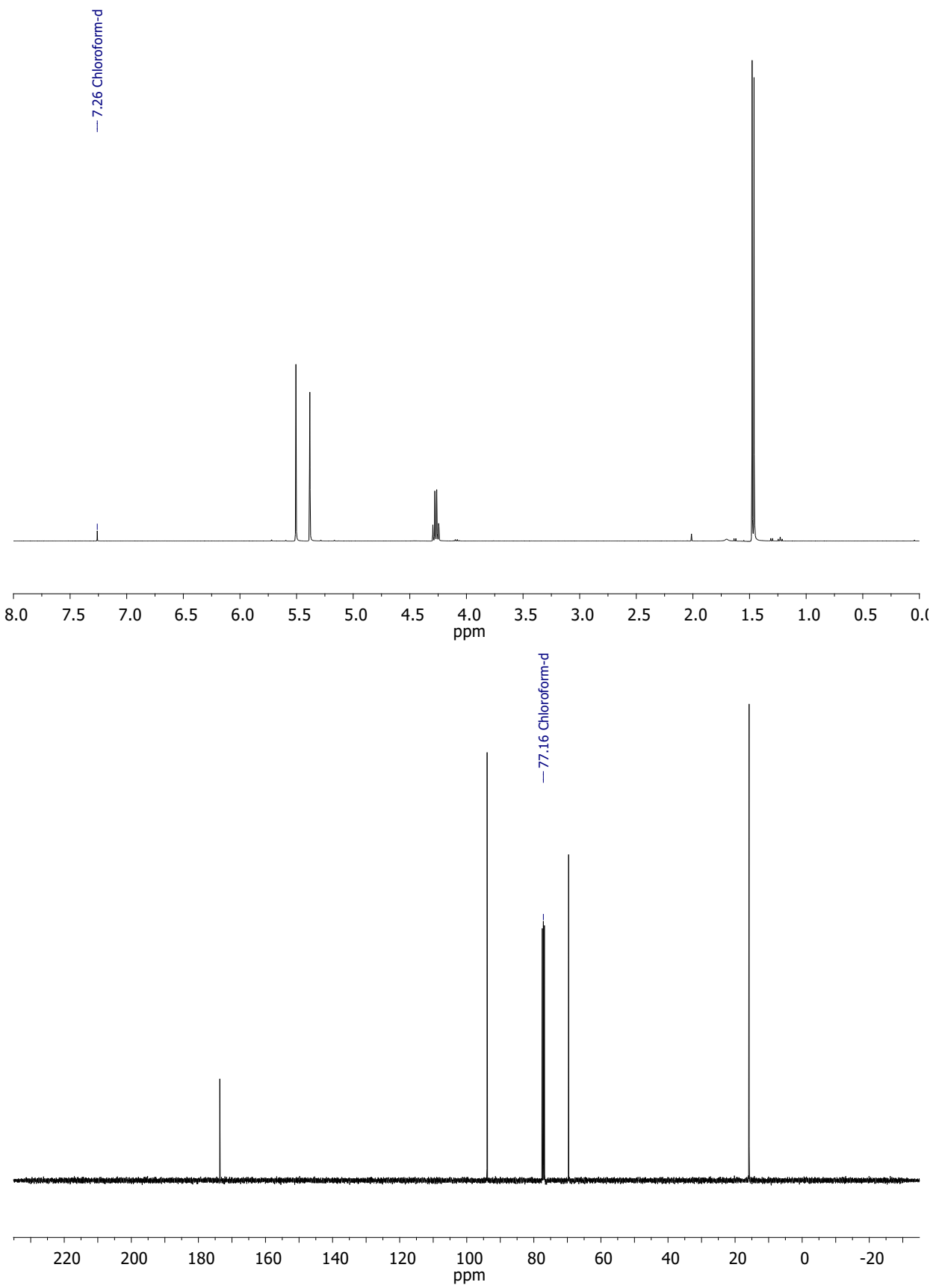


Fig. S1 ^1H NMR (top) and ^{13}C NMR (bottom) spectra of LA-H,H.

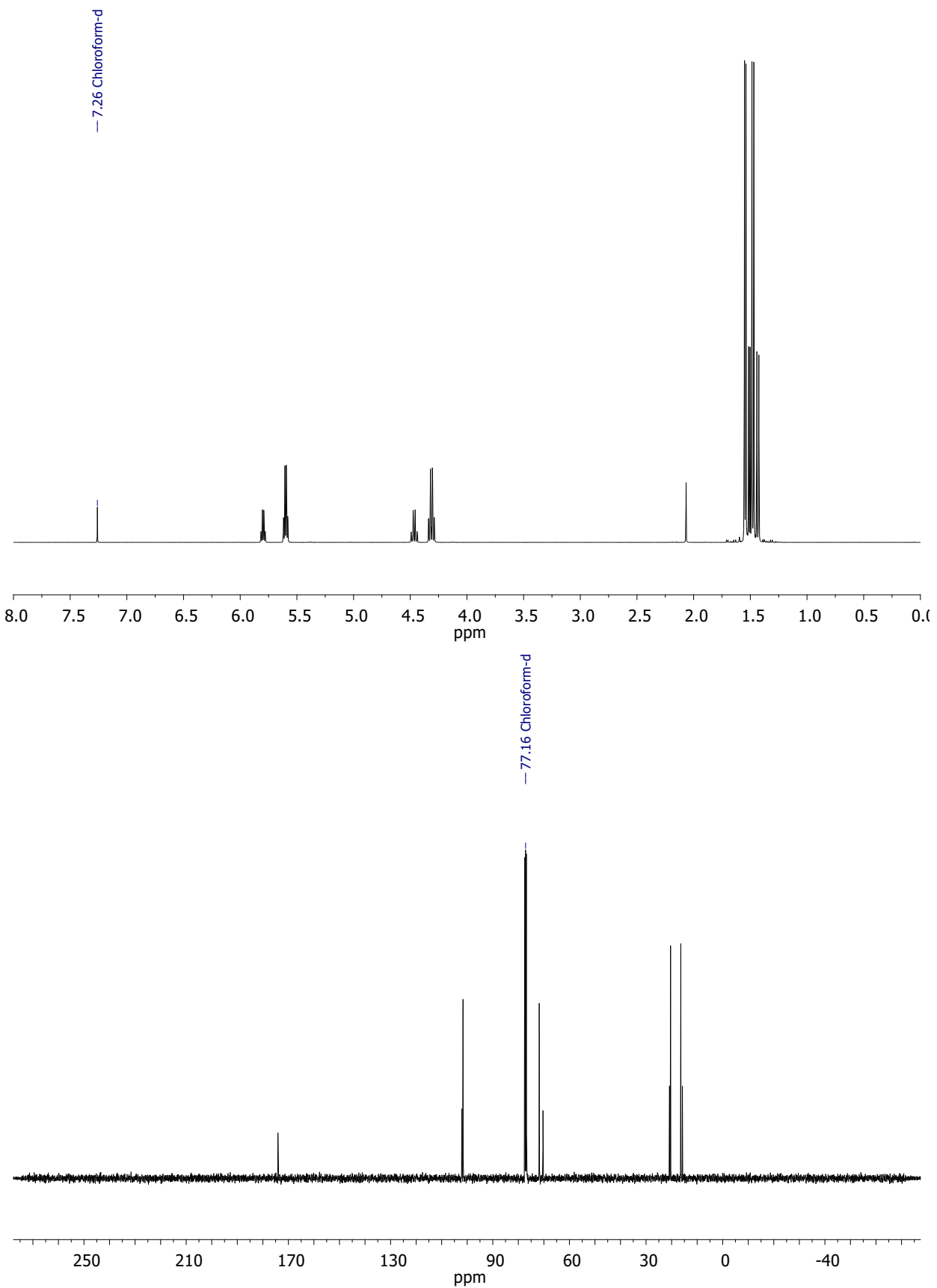


Fig. S2 ^1H NMR (top) and ^{13}C NMR (bottom) spectra of LA-H,Me. Diastereomers ratio 70:30.

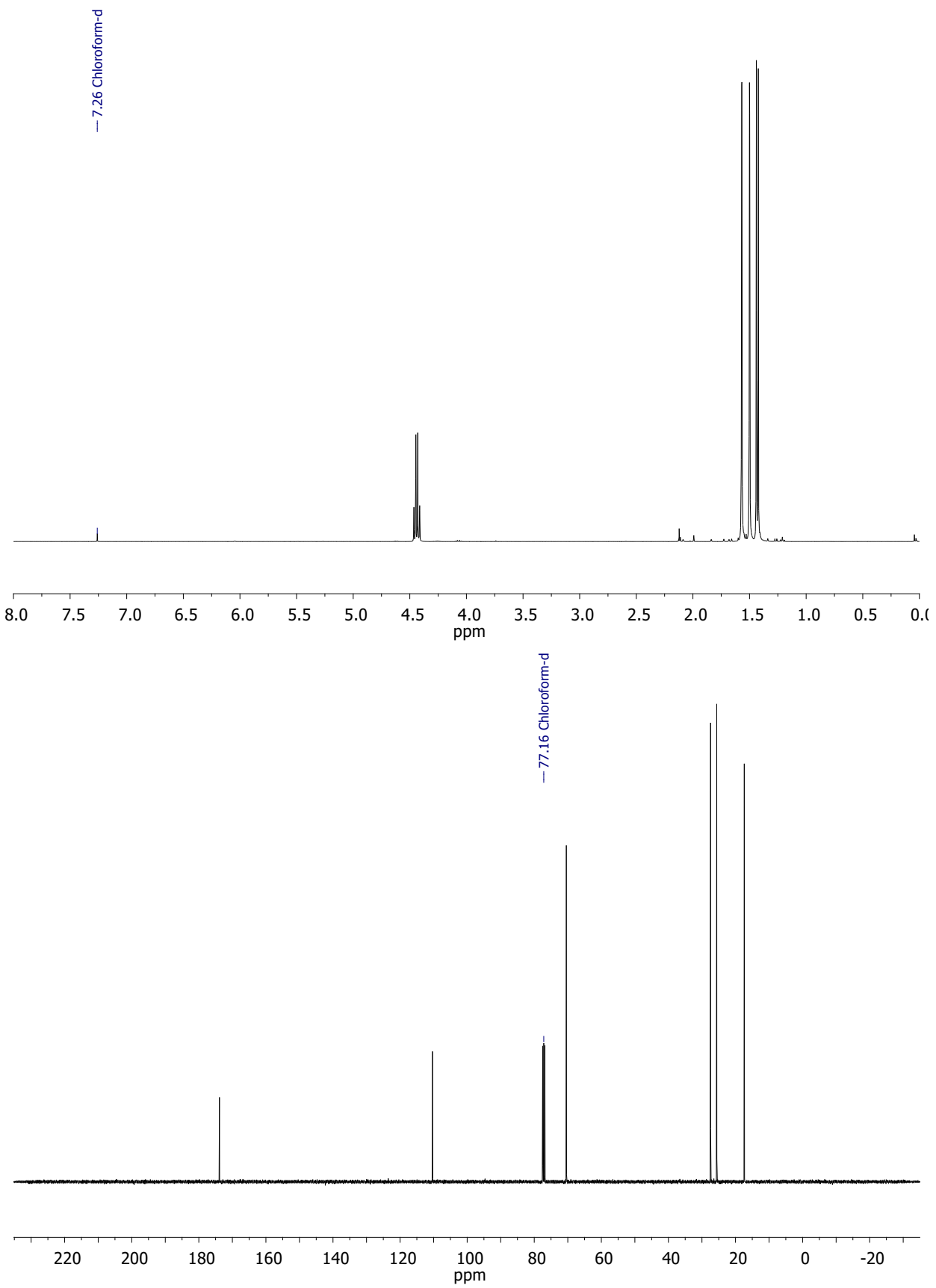


Fig. S3 ^1H NMR (top) and ^{13}C NMR (bottom) spectra of LA-Me,Me.

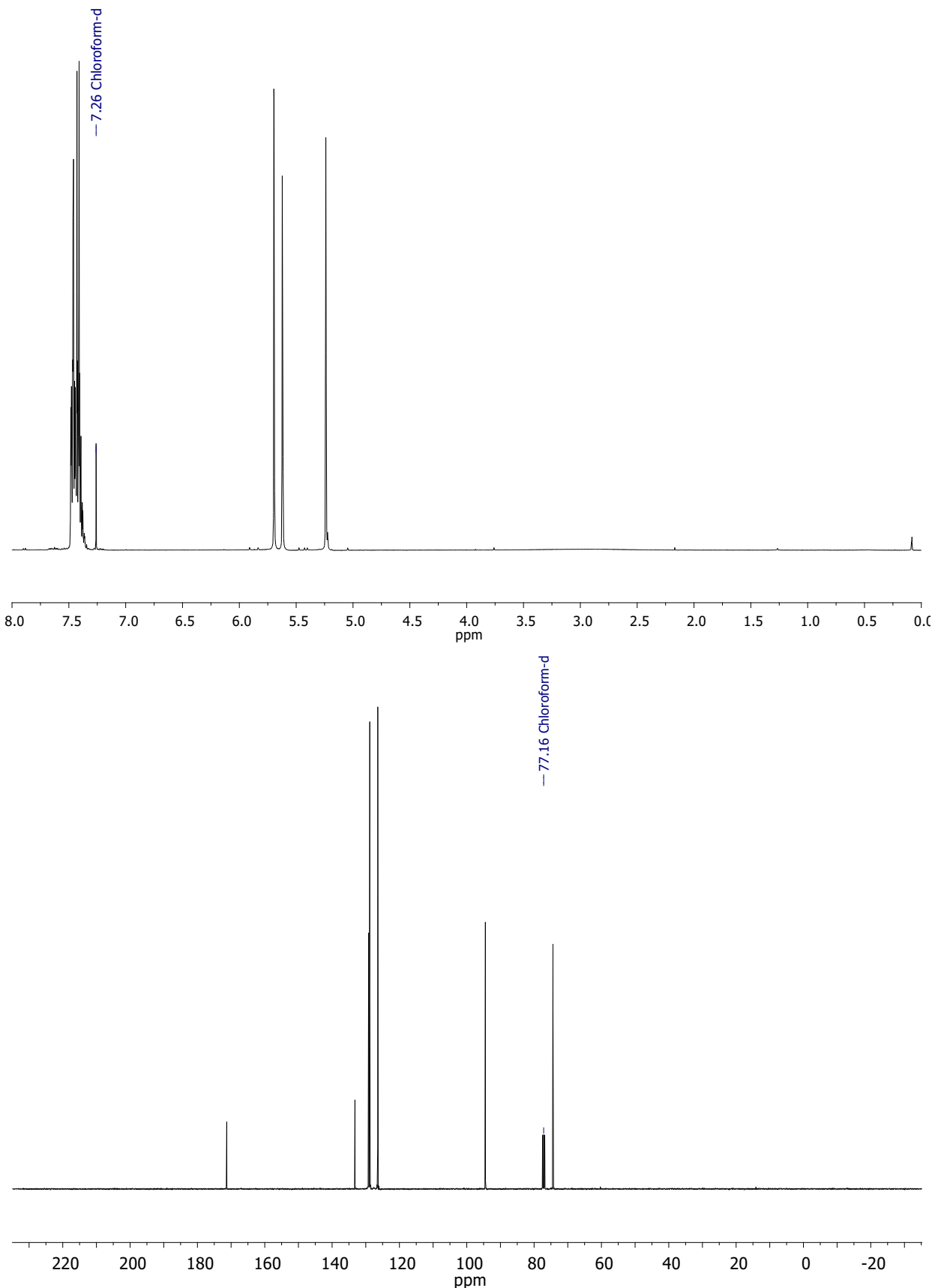


Fig. S4 ^1H NMR (top) and ^{13}C NMR (bottom) spectra of MA-H,H.

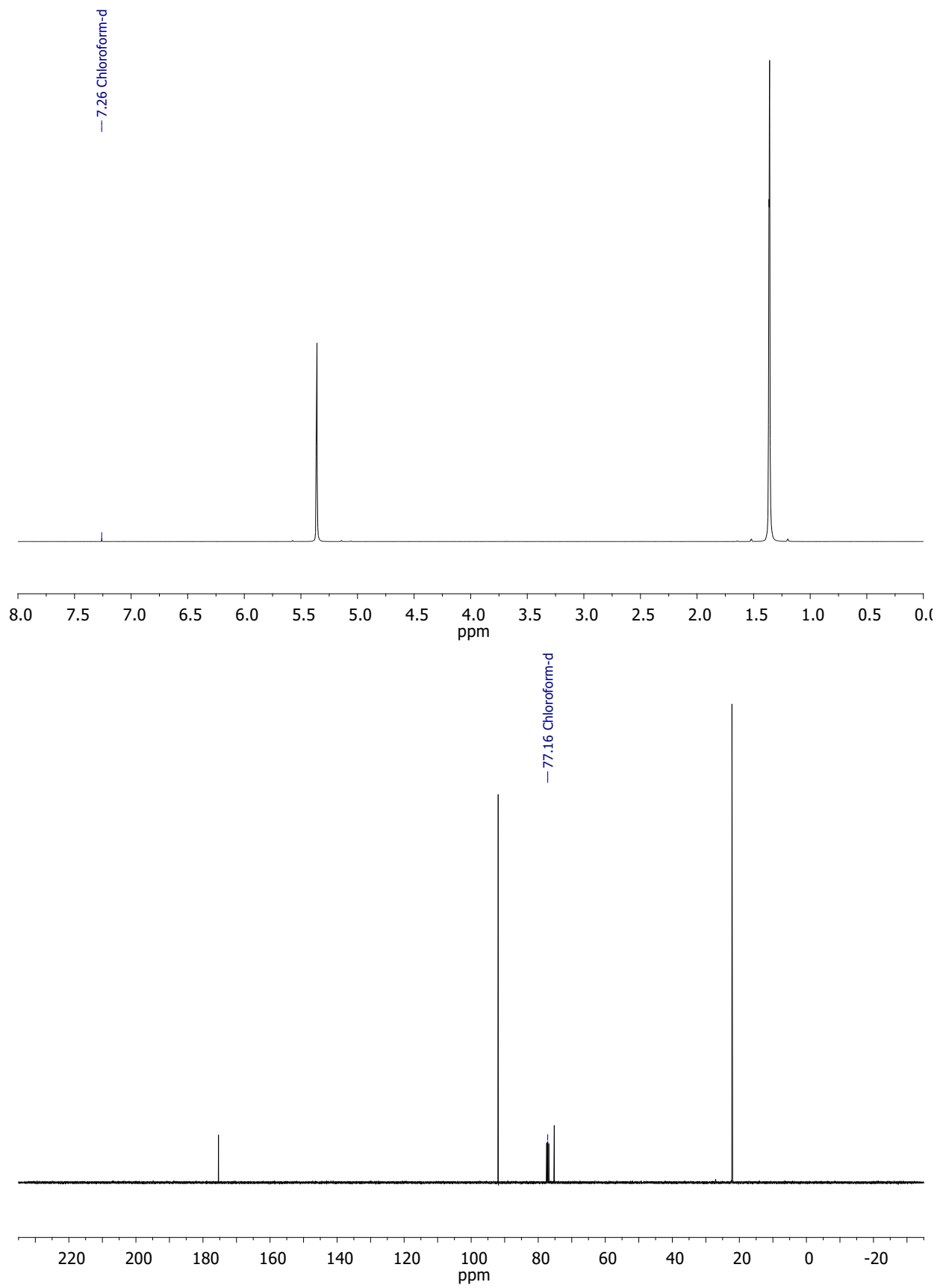


Fig. S5 ^1H NMR (top) and ^{13}C NMR (bottom) spectra of $i\text{Bu}-\text{H},\text{H}$.

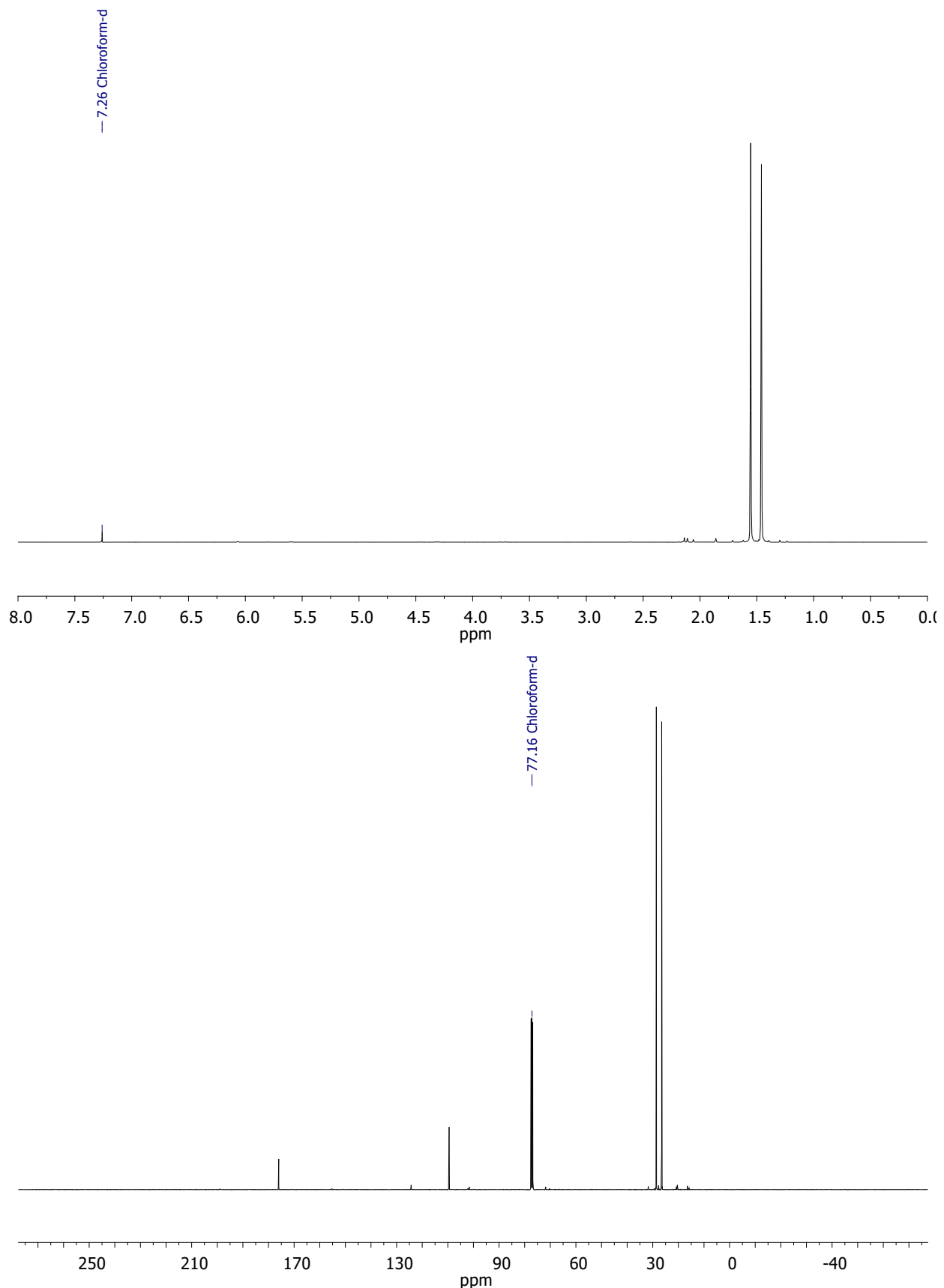


Fig. S6 ^1H NMR (top) and ^{13}C NMR (bottom) spectra of iBu-Me,Me.

Kamlet-Taft parameters determination

Hydrogen bond accepting ability¹⁰ (β) was evaluated using *p*-nitrophenol and *p*-nitroanisole as molecular probes (dyes). The complete procedure is fully described elsewhere¹¹ but is briefly reported here. Each dye was dissolved in the desired solvent (sub mM range) and the frequencies (expressed in kiloKeiser, kK, where 1 kK = 1000 cm⁻¹) of the peak at the maximum frequency (ν_{max}) were reported as abscissa (*p*-nitroanisole) and ordinate (*p*-nitrophenol). First, a calibration line was obtained using non-hydrogen accepting solvents (tetrachloroethane - TCE, dichloroethane - DCE, toluene - PhMe, and isoctane - i-C₈) and DMSO as reference hydrogen bond acceptor (excluded from the calibration line). The same procedure was used for each sample (DOXs). Calibration line and absorption frequencies of DOXs are reported in Fig. S7a and Table S2. β values for each of the DOX solvent were defined by the following equation (1):

$$(1) \quad \beta = \frac{\Delta\nu_{max(solvent)}}{\Delta\nu_{max(DMSO)}}$$

Where: $\Delta\nu_{max(solvent)}$ is the distance between the point of the solvent of interest and the linear fit of the calibration line expressed in kK; $\Delta\nu_{max(DMSO)}$ is the distance between the point of DMSO and the linear fit of the calibration curve expressed in kK. Since the ν_{max} of iBu-Me,Me fallen far from construction points of the calibration line in the aforementioned dyes, its result was discarded to avoid non-linear behaviour. Only for this solvent, the analysis was repeated using different dyes (*p*-nitroaniline and N,N-diethyl-*p*-nitroaniline) and different non-hydrogen bonding solvents (dichloroethane, DCE; dichloromethane; toluene, PhMe; *n*-hexane, *n*Hex) for the calibration line (Fig. S7b). The polarity/polarizability was evaluated by the π^* parameter.¹² This was obtained spectrophotometrically using N,N-diethylamino-4-nitroaniline (DENA) as dyes dissolved in the indicated solvents. π^* was evaluated on a scale of 0 to 1, taking the cyclohexane (CHX) as the zero value and the dimethyl sulfoxide (DMSO) as the unit value. This is defined by equation (2):

$$(2) \quad \pi^* = \frac{\nu_{max(solvent)} - \nu_{max(CHX)}}{\nu_{max(DMSO)} - \nu_{max(CHX)}}$$

Where $\nu_{max(solvent)}$, $\nu_{max(CHX)}$ and $\nu_{max(DMSO)}$ are the frequencies of the peak at maximum frequency of a solution of DENA in the studied solvent, cyclohexane and DMSO respectively, expressed in kK. Absorption frequencies of dyes in DOXs expressed in kK are collected in Table S2, while Kamlet-Taft plot (β vs π^*) of DOXs and commercial dipolar aprotic solvents are reported in Fig. 2 (main text).^T

Normalized Reichardt's polarity (E_N^T) was define with the following equation (3):^{13, 14}

$$(3) \quad E_N^T = -0.02 + 0.49\alpha + 0.38\pi^*$$

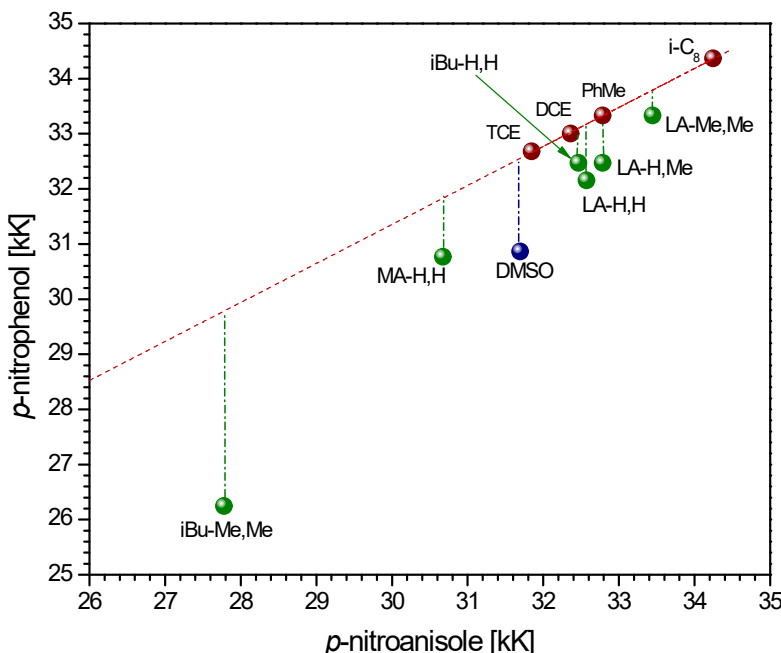


Fig. S7a Calibration line and ν_{\max} of dyes in each DOX.

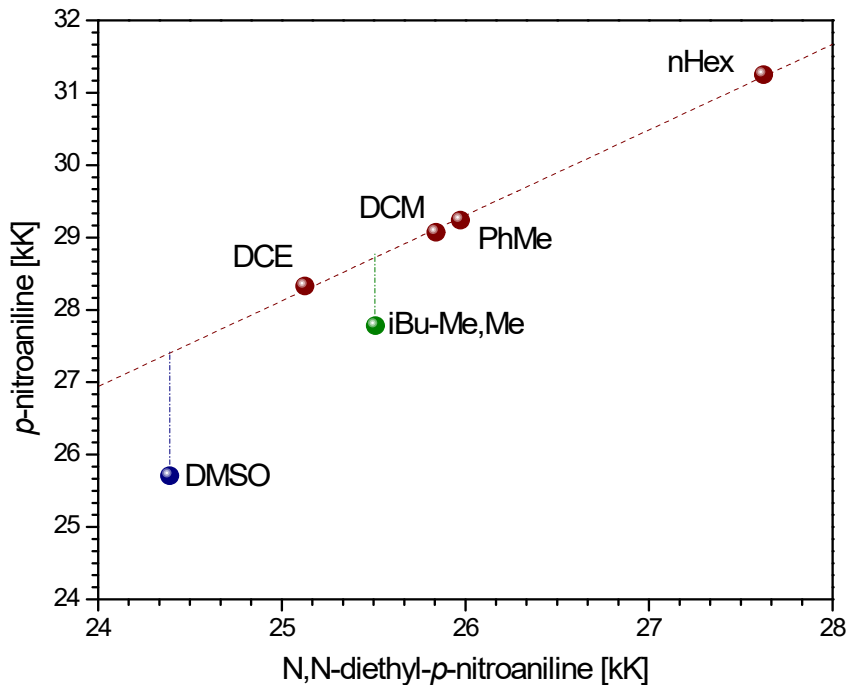


Fig. S7b Calibration line and ν_{\max} of dyes in iBu-Me,Me.

Table S2 Absorption frequencies dyes in DOXs expressed in kK.

Solvent	<i>p</i> -nitroanisole	<i>p</i> -nitrophenol	DENA	ν_{\max} [kK]
LA-H,H	32.6	32.2	24.9	
LA-H,Me	32.8	32.5	25.1	
LA-Me,Me	33.4	33.3	25.3	
MA-H,H	30.7	30.8	25.2	
iBu-H,H	32.5	32.5	25.2	
iBu-Me,Me	27.8	26.2	25.5	

Hansen and Teas parameters determination

Hansen parameters were defined by group contribution method proposed by Stefanis and Panayiotou¹⁵ using the following equations (4-7):

$$(4) \quad \delta_d = \left(\sum_i N_i C_i + W \sum_j M_j D_j + 17.3231 \right) MPa^{\left(\frac{1}{2}\right)}$$

$$(5) \quad \delta_p = \left(\sum_i N_i C_i + W \sum_j M_j D_j + 7.3548 \right) MPa^{\left(\frac{1}{2}\right)}$$

$$(6) \quad \delta_{hb} = \left(\sum_i N_i C_i + W \sum_j M_j D_j + 7.9793 \right) MPa^{\left(\frac{1}{2}\right)}$$

$$(7) \quad \delta_t = \left(\sqrt{\delta_d^2 + \delta_p^2 + \delta_{hb}^2} \right) MPA^{\frac{1}{2}}$$

Where C_i and D_j are respectively the first- and second-order contribution of type i and j that appears N_i and M_j times in the compound structure and are listed in the original papers. The constant W is equal to 1 or 0 for compound with or without second-order order groups. Group contribution factors for the DOXs are collected in **Tables S3-S8**. Results are graphically represented in the 3D Hansen space in **Fig. S8**. Distances (R_a) between DOXs ($\delta_{d1}, \delta_{p1}, \delta_{hb1}$) and commercial polar aprotic solvents or polymers ($\delta_{d2}, \delta_{p2}, \delta_{hb2}$) in the 3D Hansen space were defined with equation (8) and reported in **Tables 2** and **S9**. Relative Energy Differences (REDs) between DOXs and common polymers (**Table S10**) were calculated using equations (9) and reported in **Table S11**.

$$(8) \quad R_a = \sqrt{4(\delta_{d1} - \delta_{d2})^2 + (\delta_{p1} - \delta_{p2})^2 + (\delta_{hb1} - \delta_{hb2})^2}$$

$$(9) \quad RED = \frac{R_a}{R_0}$$

Where R_0 is the radius of the Hansen solubility parameter for each polymer: $RED < 1$ indicates good solvents, $RED > 1$ indicates poor solvents

Table S3 Hansen parameters for LA-H,H defined with Stefanis group contribution method.

LA-H,H									
Group I Order	N°	δ_d	δ_p	δ_{hb}	Group II Order	N°	δ_d	δ_p	δ_{hb}
-CH ₃	1	-0.9714	-1.6448	-0.7813	String in cyclic	1	-0.1945		
-CH ₂	1	-0.0269	-0.3045	-0.4119	Ocyclic-Cyclic=O	1	0.2468	2.7501	0.122
-CH<	1	0.645	0.6491	-0.2018					
>C<	0	1.2686	2.0838	0.0866					
ACH	0	0.1105	-0.5303	-0.4305					
					δ_d	17.5			
					δ_p	13.5			
COO	1	0.2039	3.4637	1.1389	δ_{hb}	8.7			
CH ₂ O (cyclic)	1	0.2753	0.1994	-0.161	δ_t	23.7			
	C _i	17.3231	7.3548	7.9793					

Table S4 Hansen parameters for LA-H,Me defined with Stefanis group contribution method.

LA-H,Me									
Group I Order	N°	δ_d	δ_p	δ_{hb}	Group II Order	N°	δ_d	δ_p	δ_{hb}
-CH ₃	2	-0.9714	-1.6448	-0.7813	String in cyclic	2	-0.1945		
-CH ₂	0	-0.0269	-0.3045	-0.4119	Ocyclic-Cyclic=O	1	0.2468	2.7501	0.122
-CH<	2	0.645	0.6491	-0.2018					
>C<	0	1.2686	2.0838	0.0866					
ACH	0	0.1105	-0.5303	-0.4305					
					δ_d	17.0			
					δ_p	12.8			
COO	1	0.2039	3.4637	1.1389	δ_{hb}	8.1			
CH ₂ O (cyclic)	1	0.2753	0.1994	-0.161	δ_t	22.8			
	C _i	17.3231	7.3548	7.9793					

Table S5 Hansen parameters for LA-Me,Me defined with Stefanis group contribution method.

LA-Me,Me									
Group I Order	N°	δ_d	δ_p	δ_{hb}	Group II Order	N°	δ_d	δ_p	δ_{hb}
-CH ₃	3	-0.9714	-1.6448	-0.7813	String in cyclic	3	-0.1945		
-CH ₂	0	-0.0269	-0.3045	-0.4119	Ocyclic-Cyclic=O	1	0.2468	2.7501	0.122
-CH<	1	0.645	0.6491	-0.2018					
>C<	1	1.2686	2.0838	0.0866					
ACH	0	0.1105	-0.5303	-0.4305					
					δ_d	16.5			
					δ_p	12.6			
COO	1	0.2039	3.4637	1.1389	δ_{hb}	7.6			
CH ₂ O (cyclic)	1	0.2753	0.1994	-0.161	δ_t	22.1			
	C _i	17.3231	7.3548	7.9793					

Table S6 Hansen parameters for MA-H,H defined with Stefanis group contribution method.

MA-H,H									
Group I Order	N°	δ_d	δ_p	δ_{hb}	Group II Order	N°	δ_d	δ_p	δ_{hb}
-CH ₃	0	-0.9714	-1.6448	-0.7813	String in cyclic	1	-0.1945		
-CH ₂	1	-0.0269	-0.3045	-0.4119	Ocyclic-Cyclic=O	1	0.2468	2.7501	0.122
-CH<	1	0.645	0.6491	-0.2018					
>C<	0	1.2686	2.0838	0.0866					
ACH	5	0.1105	-0.5303	-0.4305					
ACCH	1	0.6933	0.6517	-0.1375	δ_d	19.0			
					δ_p	12.5			
COO	1	0.2039	3.4637	1.1389	δ_{hb}	7.2			
CH ₂ O (cyclic)	1	0.2753	0.1994	-0.161	δ_t	23.8			
C _i	17.3231	7.3548	7.9793						

Table S7 Hansen parameters for iBu-H,H defined with Stefanis group contribution method.

iBu-H,H									
Group I Order	N°	δ_d	δ_p	δ_{hb}	Group II Order	N°	δ_d	δ_p	δ_{hb}
-CH ₃	2	-0.9714	-1.6448	-0.7813	String in cyclic	2	-0.1945		
-CH ₂	1	-0.0269	-0.3045	-0.4119	Ocyclic-Cyclic=O	1	0.2468	2.7501	0.122
-CH<	0	0.645	0.6491	-0.2018					
>C<	1	1.2686	2.0838	0.0866					
ACH	0	0.1105	-0.5303	-0.4305					
					δ_d	17.0			
					δ_p	13.3			
COO	1	0.2039	3.4637	1.1389	δ_{hb}	8.2			
CH ₂ O (cyclic)	1	0.2753	0.1994	-0.161	δ_t	23.0			
C _i	17.3231	7.3548	7.9793						

Table S8 Hansen parameters for iBu-Me,Me defined with Stefanis group contribution method.

iBu-Me,Me									
Group I Order	N°	δ_d	δ_p	δ_{hb}	Group II Order	N°	δ_d	δ_p	δ_{hb}
-CH ₃	4	-0.9714	-1.6448	-0.7813	String in cyclic	4	-0.1945		
-CH ₂	0	-0.0269	-0.3045	-0.4119	Ocyclic-Cyclic=O	1	0.2468	2.7501	0.122
-CH<	0	0.645	0.6491	-0.2018					
>C<	2	1.2686	2.0838	0.0866					
ACH	0	0.1105	-0.5303	-0.4305					
					δ_d	17.0			
					δ_p	12.8			
COO	1	0.2039	3.4637	1.1389	δ_{hb}	8.1			
CH ₂ O (cyclic)	1	0.2753	0.1994	-0.161	δ_t	22.8			
C _i	17.3231	7.3548	7.9793						

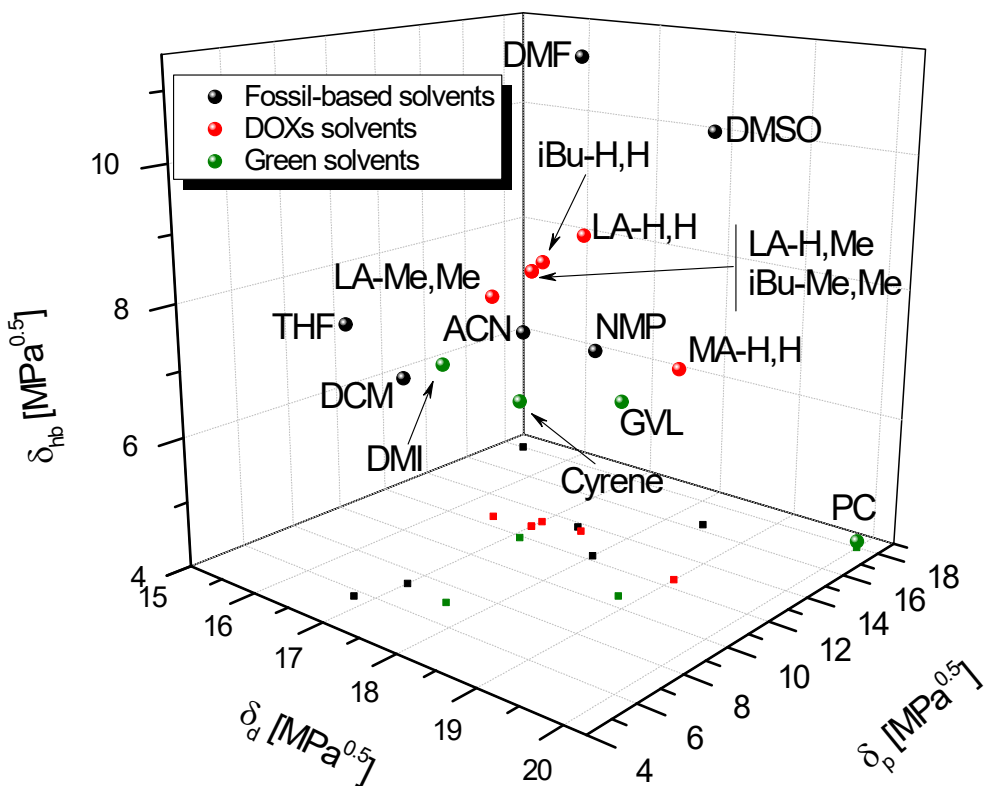


Fig. S8 3D Hansen space for fossil-based (black), green (green), and DOXs (red) solvents. LA-H,Me and iBu-Me,Me overlaps.

Table S9. Distance in tridimensional Hansen space among commercial polar aprotic solvents and DOXs solvents. ACN, acetonitrile; DCM, dichloromethane; DMF, dimethylformamide; DMSO, dimethylsulphoxide; NMP, N-methyl pyrrolidone; THF, tetrahydrofurane; PC, propylene carbonate; DMI, dimethyl isosorbide; GVL, γ -valerolactone. Data with $R_a < 5$ are marked in bold.

	$R_a(LA-H,H)$	$R_a(LA-H,Me)$	$R_a(LA-Me,Me)$	$R_a(MA-H,H)$	$R_a(iBu-H,H)$	$R_a(iBu-Me,Me)$	$R_a(GVL)$
Acetone	14.3	8.0	4.6	26.7	9.4	8.0	3.6
ACN	23.2	21.3	18.6	43.1	19.0	21.3	7.1
DCM	21.0	15.6	14.7	21.5	18.6	15.6	4.7
DMF	3.4	5.8	9.1	14.2	5.2	5.8	5.4
DMSO	6.9	12.6	17.8	12.8	10.7	12.6	6.6
NMP	2.3	2.5	4.6	2.0	3.0	2.5	2.1
THF	31.6	25.3	24.1	33.1	29.0	25.3	6.5
PC	33.2	39.5	45.2	21.9	37.5	39.5	8.7
DMI	21.2	17.1	17.6	18.5	20.2	17.1	5.1
Cyrene™	9.2	9.6	12.8	1.9	11.0	9.6	3.7
GVL	4.7	2.2	1.9	7.9	3.0	2.2	-

Table S10 Hansen parameters of common polymers used to calculate RED vs DOXs solvents.

Polymers	δ_d	δ_p	δ_h	R_0	Ref
Pet	18.2	6.4	6.6	8	¹⁶
Nylon 66	17.4	9.9	14.6	8	¹⁶
Epoxy resin	17.4	10.5	9	8	¹⁶
Polyvinylbutyral	18.6	4.4	13	8	¹⁶
Polyvinylidenefluoride (PVF)	17	12.1	10.2	8	¹⁶
Polyphenyleneoxide (PPO)	17.9	3.1	8.5	8	¹⁶
Polyurethane (PU)	18.1	9.3	4.5	8	¹⁶
Polysulphone	16	6	6.6	8	¹⁶
Polysilicone	17.2	3	3	8	¹⁶
Polyethersulphone	19	11	8	8	¹⁶
Polyoxymethylene (POM)	17.2	9.2	9.8	8	¹⁶
Polyvinylpyrrolidone (PVP)	18.1	10	18	8	¹⁶
Cyclic olefin copolymer (COC)	18	3	2	8	¹⁶
Polyethylene oxide (PEO)	17	10	5	8	¹⁶
Polypropylene oxide (PPO)	16.5	9	7	8	¹⁶
Polyvinyl alcohol (PVOH)	15	17.2	17.8	8	¹⁶
Polylactic acid (PLA)	18.5	8	7	8	¹⁶
Finntalc m15 (mondo minerals)	17.89	8.29	10.34	5.3	¹⁶
Lignina	21.9	14.1	16.9	13.7	¹⁷
Dextran C	24.3	19.9	22.5	17.4	¹⁷
Methyl cellulose	17.1	9.8	13.2	10.2	¹⁷
Sucrose	23.4	18.4	20.8	16	¹⁷
Natural rubber (gloves)	16.4	3.1	4.1	6.8	¹⁸
Nitrile (gloves)	20.4	12.4	4.1	13.9	¹⁸
Butyl (gloves)	17.3	1.4	2.6	6.3	¹⁸
Neoprene (gloves)	19.2	3.9	3.9	10.2	¹⁸
Viton (gloves)	15.6	11.3	5.4	7.9	¹⁸

Table S11 Relative energy difference (RED) between common polymers and DOXs solvents. When RED < 1 the affinity between solvents and polymer is high. Data with RED < 1 are marked in bold.

Polymers	RED					
	[LA-H,H]	[LA-H,Me]	[LA-Me,Me]	[iBu-Me,Me]	[iBu-H,H]	[iBu-Me,Me]
PET	0.94	0.87	0.89	0.87	0.93	0.79
Nylon 66	0.86	0.90	0.96	0.90	0.91	1.06
Epoxy resin	0.38	0.32	0.39	0.32	0.38	0.52
Polyvinylbutyral	1.29	1.28	1.33	1.28	1.33	1.25
Polyvinylidenefluoride (PVF)	0.29	0.28	0.35	0.28	0.29	0.63
Polyphenyleneoxide (PPO)	1.30	1.23	1.24	1.23	1.30	1.22
Polyurethane (PU)	0.76	0.69	0.69	0.69	0.73	0.57
Polysulphone	1.04	0.91	0.84	0.91	0.97	1.11
Polysilicone	1.50	1.38	1.34	1.38	1.44	1.37
Polyethersulphone	0.50	0.55	0.66	0.55	0.58	0.21
Polyoxymethylene (POM)	0.56	0.50	0.54	0.50	0.55	0.69
Polyvinylpyrrolidone (PVP)	1.25	1.32	1.40	1.32	1.32	1.40
Cyclic olefin copolymer (COC)	1.56	1.46	1.44	1.46	1.52	1.38
Polyethylene oxide (PEO)	0.65	0.52	0.48	0.52	0.57	0.65
Polypropylene oxide (PPO)	0.65	0.51	0.46	0.51	0.57	0.76
Polyvinyl alcohol (PVOH)	1.38	1.42	1.45	1.42	1.39	1.76
Polylactic acid (PLA)	0.76	0.72	0.77	0.72	0.78	0.58
Finntalc m15 (mondo minerals)	1.04	1.01	1.10	1.01	1.08	1.08
Lignina	0.88	0.97	1.05	0.97	0.96	0.83
Dextran C	1.17	1.25	1.31	1.25	1.23	1.15
Methyl cellulose	0.58	0.58	0.62	0.58	0.60	0.74
Sucrose	1.10	1.18	1.25	1.18	1.17	1.08
Natural rubber (gloves)	1.70	1.55	1.49	1.55	1.63	1.64
Nitrile (gloves)	0.54	0.57	0.62	0.57	0.57	0.30
Butyl (gloves)	2.15	2.01	1.96	2.01	2.09	1.98
Neoprene (gloves)	1.10	1.06	1.07	1.06	1.10	0.90
Viton (gloves)	0.70	0.53	0.40	0.53	0.56	0.90

Teas parameters were obtained with the following equations (10-12) and displayed in Fig. S9.

$$(10) \quad F_d = \frac{100\delta_d}{\delta_d + \delta_p + \delta_{hb}}$$

$$(11) \quad F_p = \frac{100\delta_p}{\delta_d + \delta_p + \delta_{hb}}$$

$$(12) \quad F_{hb} = \frac{100\delta_{hb}}{\delta_d + \delta_p + \delta_{hb}}$$

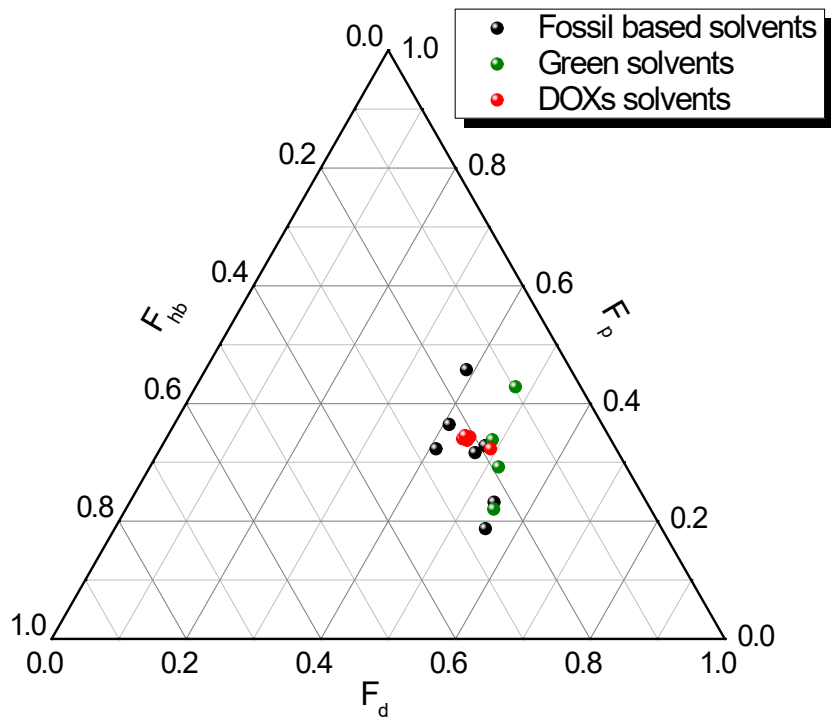


Fig. S9 Teas plot representation of fossil-based (black), green (green) and DOXs (red) solvents.

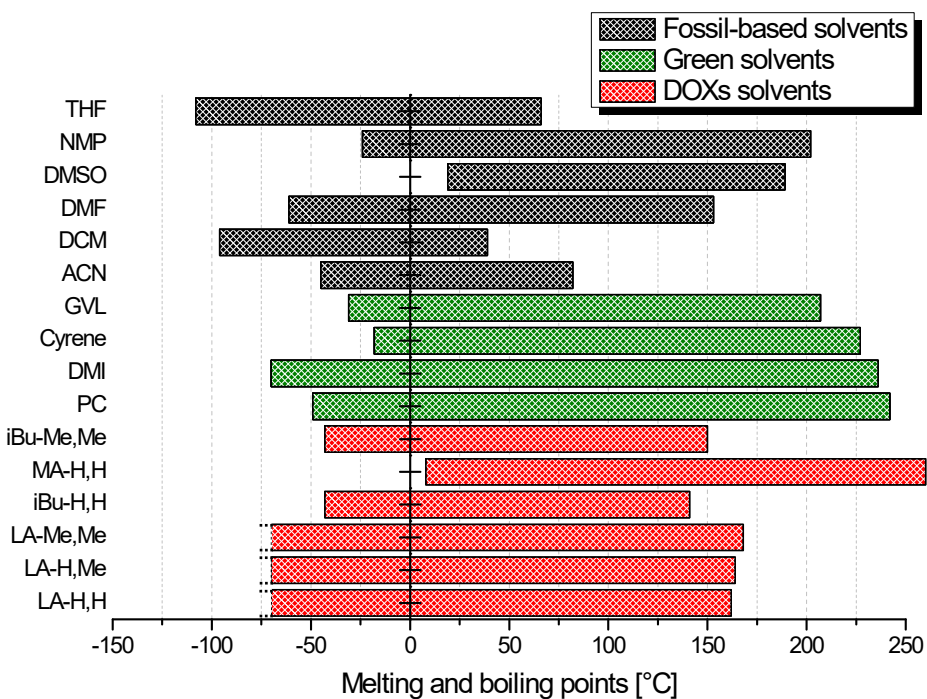


Fig. S10 Thermal liquid range (mp and bp) at ambient pressure of DOXs and commercial polar aprotic solvents (green and fossil based). Melting point for LA-X,X are below -70 °C.

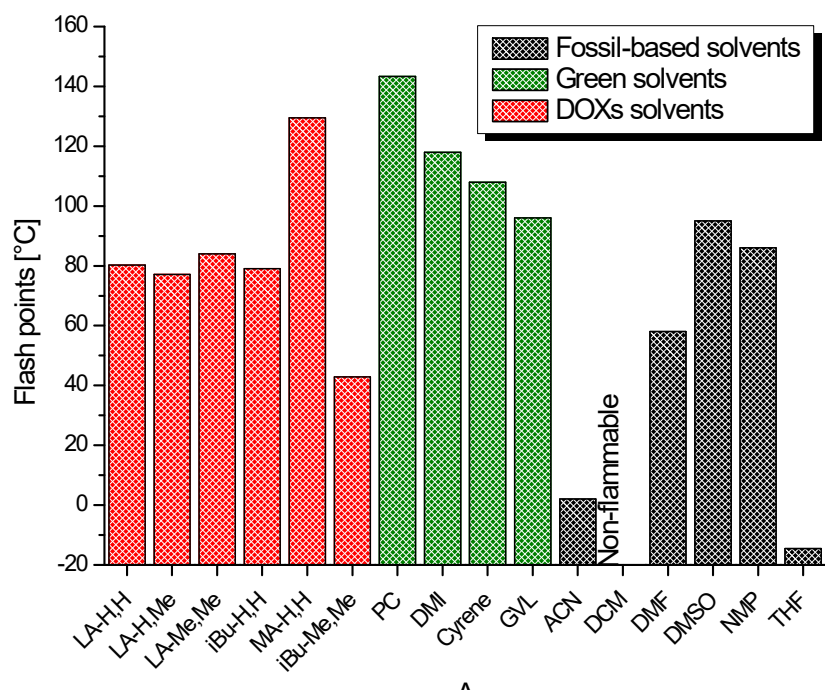


Fig. S11 Flash points of DOXs and commercial polar aprotic solvents (green and fossil based).

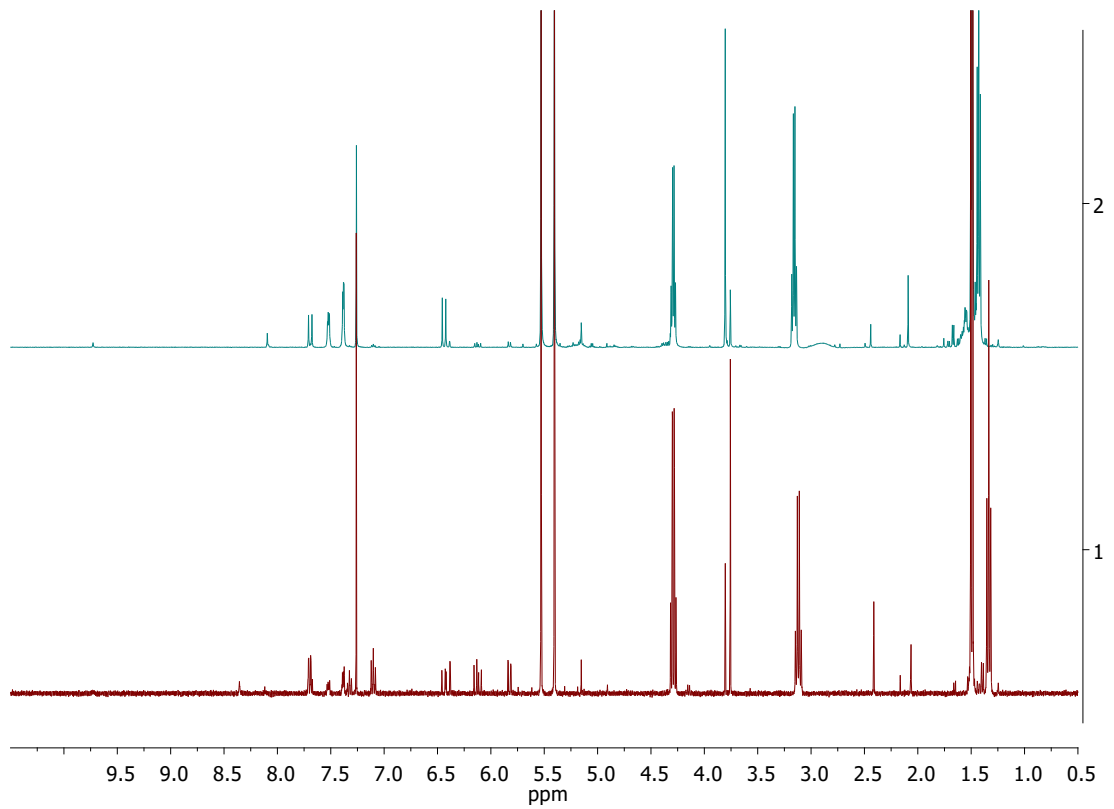


Fig. S12 Mizoroki-Heck coupling in LA-H,H. Traces 1 (0.5 h) and 2 (24 h) of Table 3 Entry 1

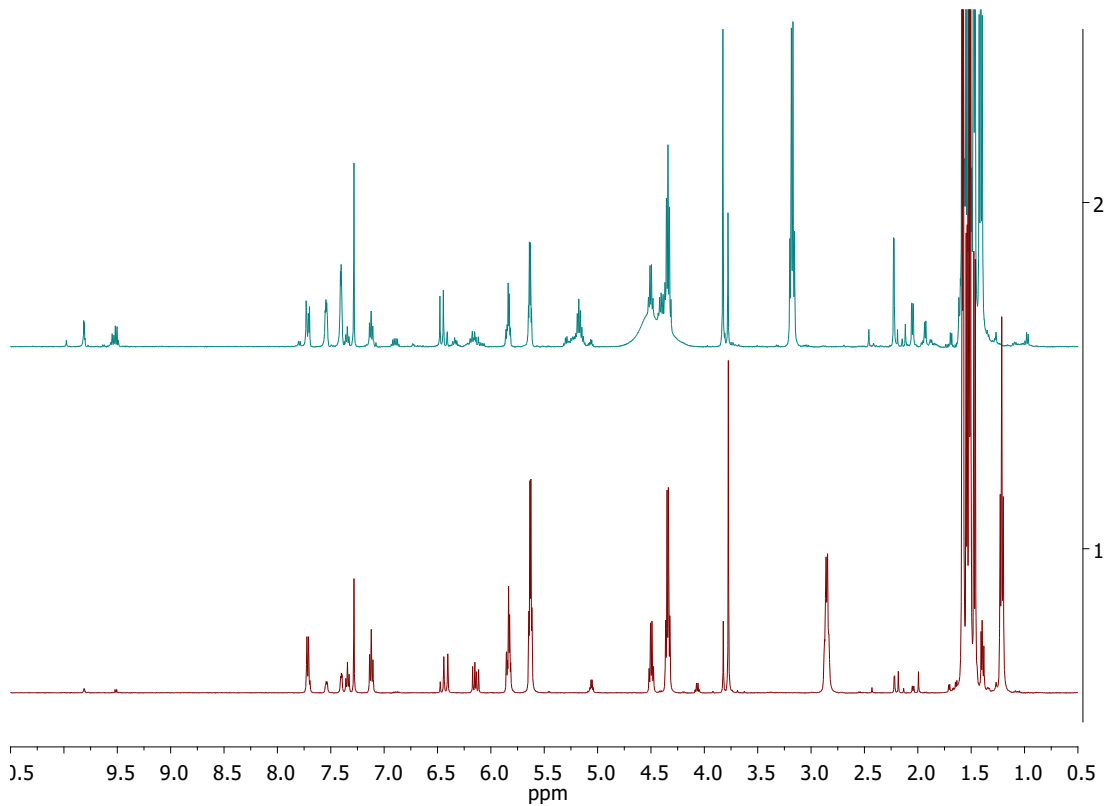


Fig. S13. Mizoroki-Heck coupling in LA-H,Me. Traces 1 (0.5 h) and 2 (24 h) of Table 3 Entry 2.

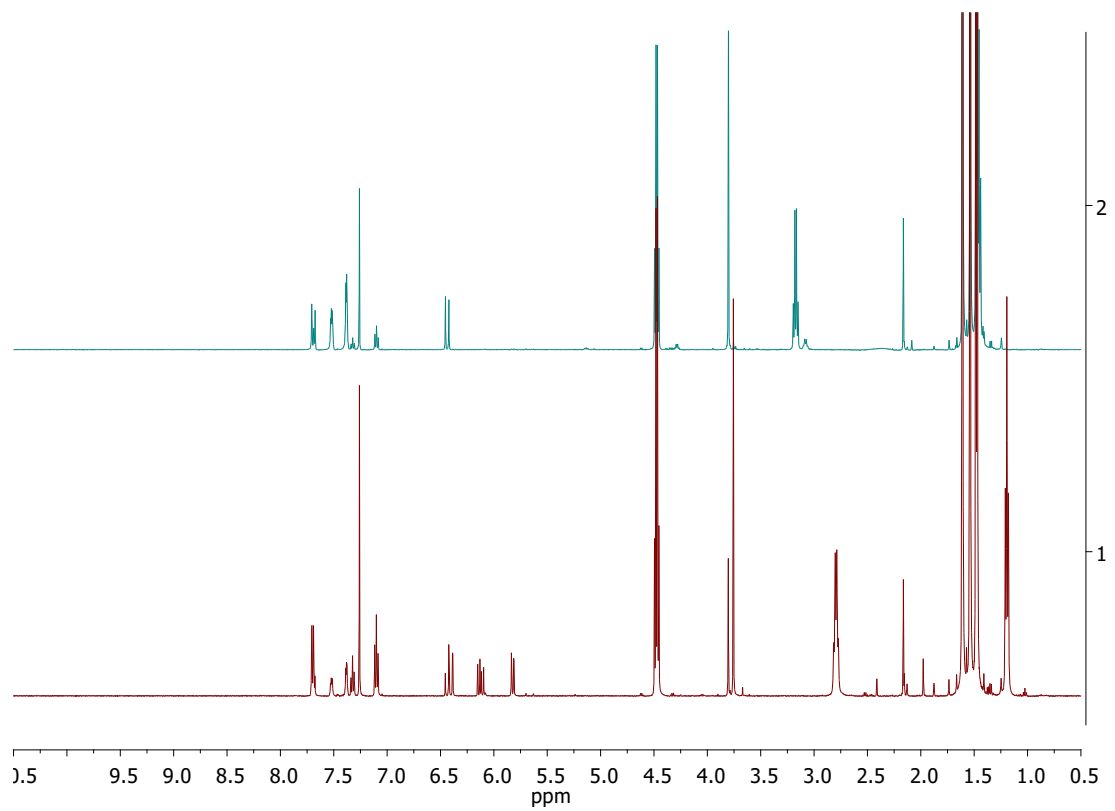


Fig. S14 Mizoroki-Heck coupling in LA-Me,Me. Traces 1 (0.5 h) and 2 (24 h) of Table 3 Entry 3.

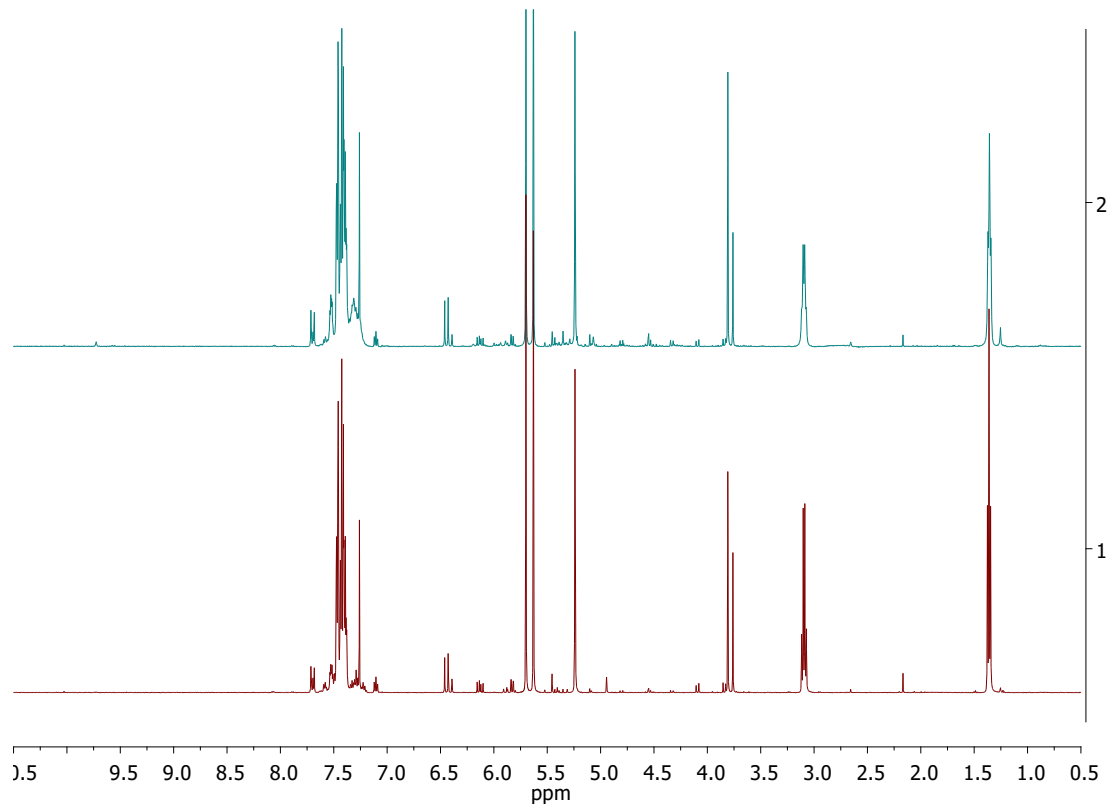


Fig. S15 Mizoroki-Heck coupling in MA-H,H. Traces 1 (0.5 h) and 2 (24 h) of Table 3 Entry 4

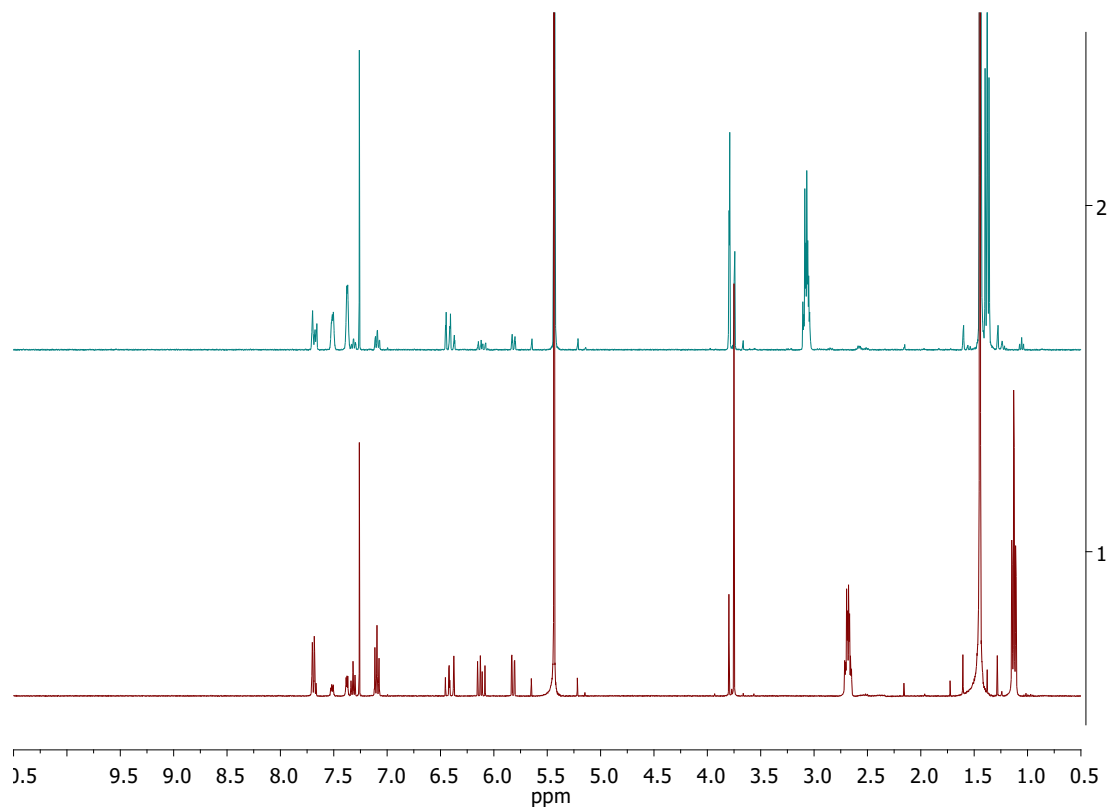


Fig. S16 Mizoroki-Heck coupling in iBu-H,H. Traces 1 (0.5 h) and 2 (24 h) of Table 3 Entry 5

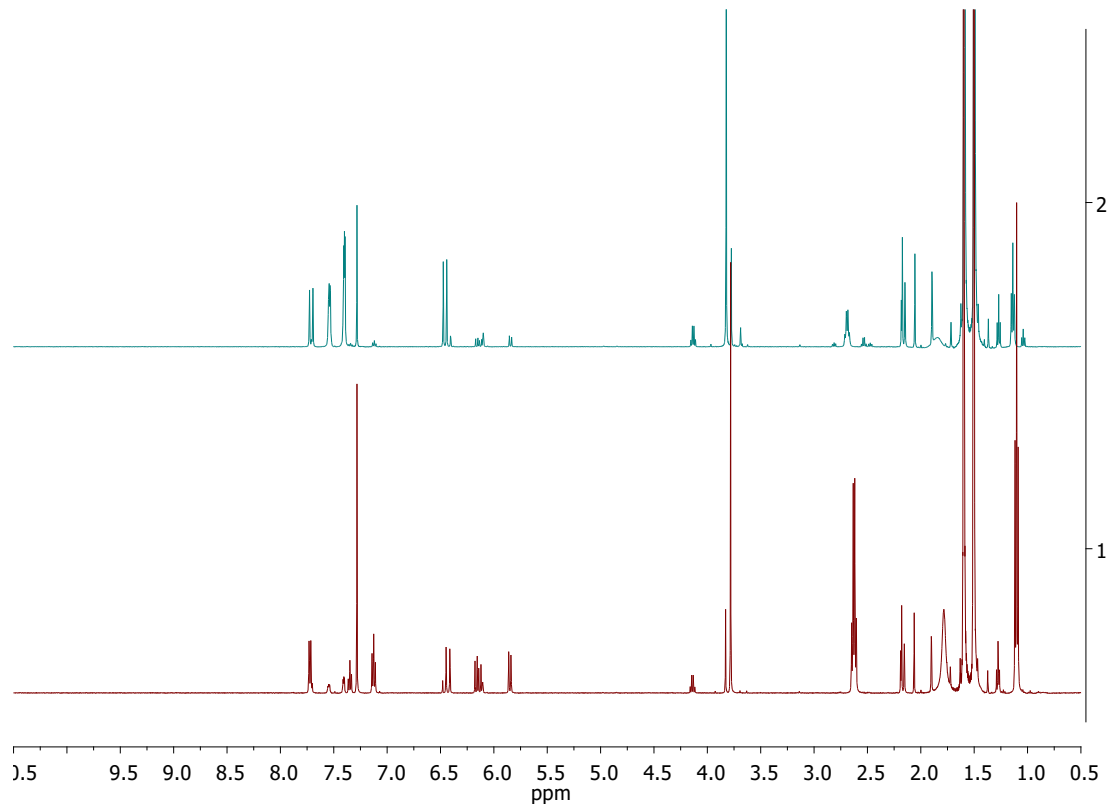


Fig. S17 Mizoroki-Heck coupling in iBu-Me,Me. Traces 1 (0.5 h) and 2 (24 h) of Table 3 Entry 6.

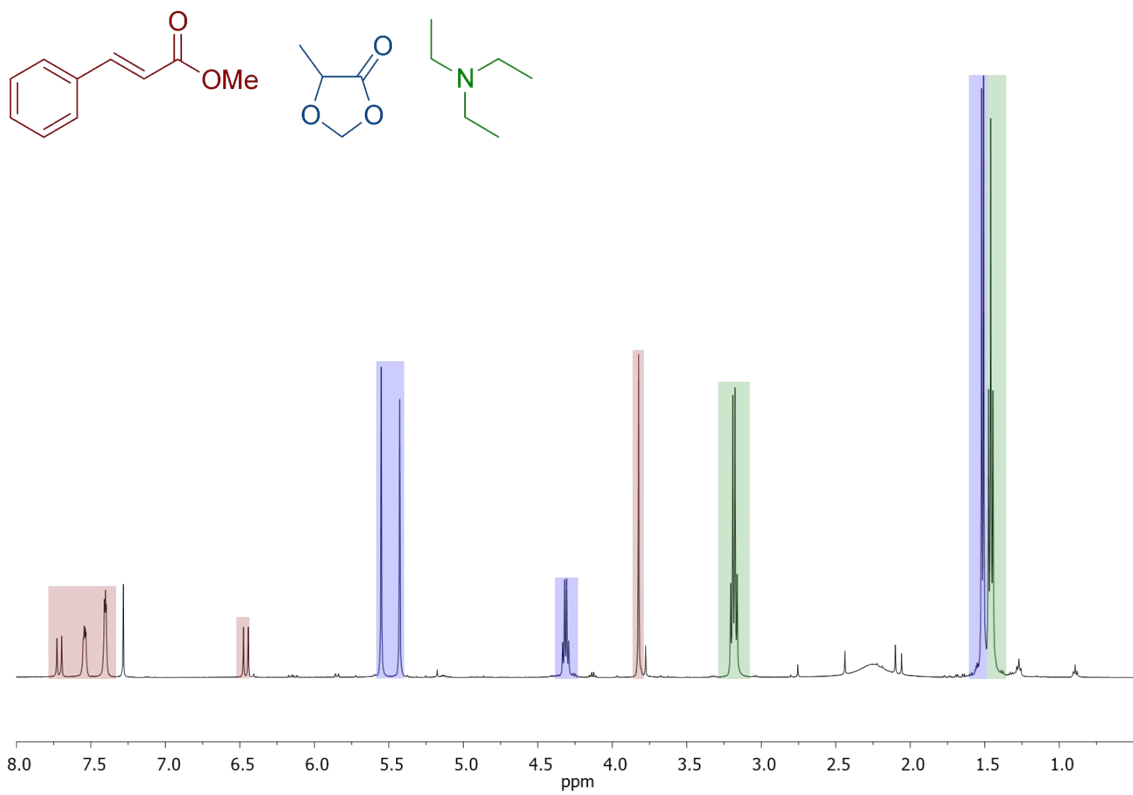


Fig. S18. ¹H NMR signal assignment of Mizoroki-Heck reaction mixture in LA-H,H.

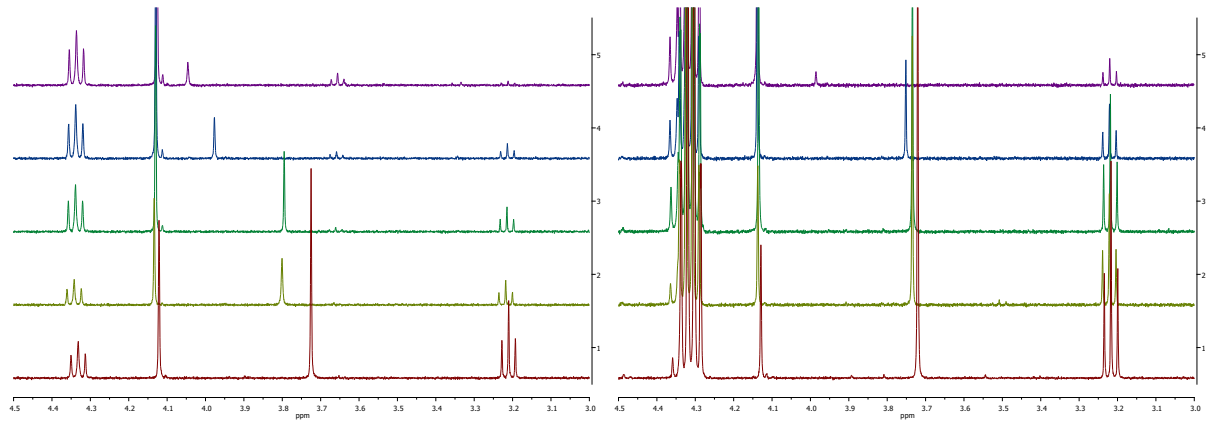


Fig. S19. Relevant portion of ¹H NMR of Menschutkin reaction in DMSO (left) and LA-H,H (right). Trace 1, 2, 3, 4, 5 represent crude reaction mixture at different time: 0.5 (bottom), 1, 2, 4, 24 (top) hours.

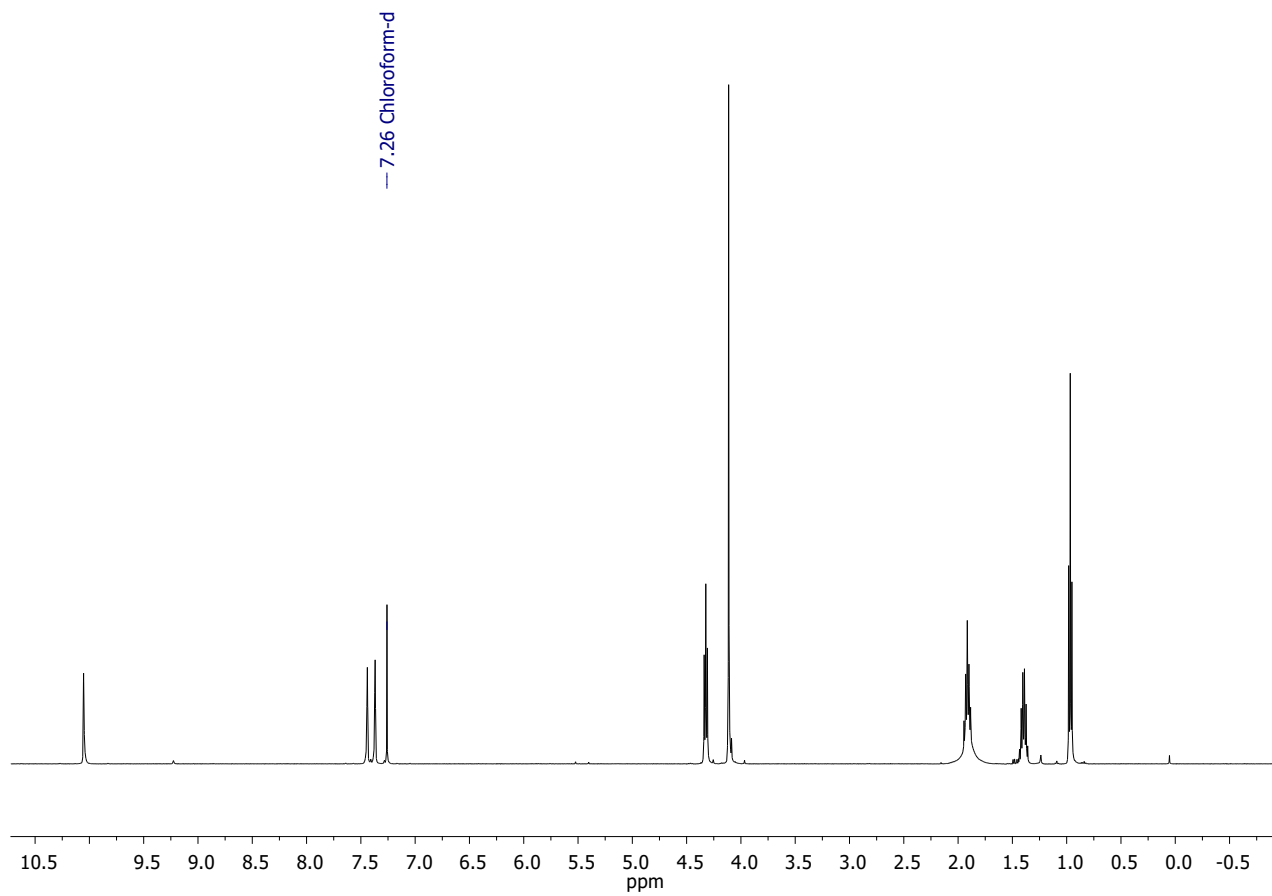


Fig. S20 ^1H NMR of 1-butyl-3-methyl-imidazolium iodide isolated from LA-H,H.

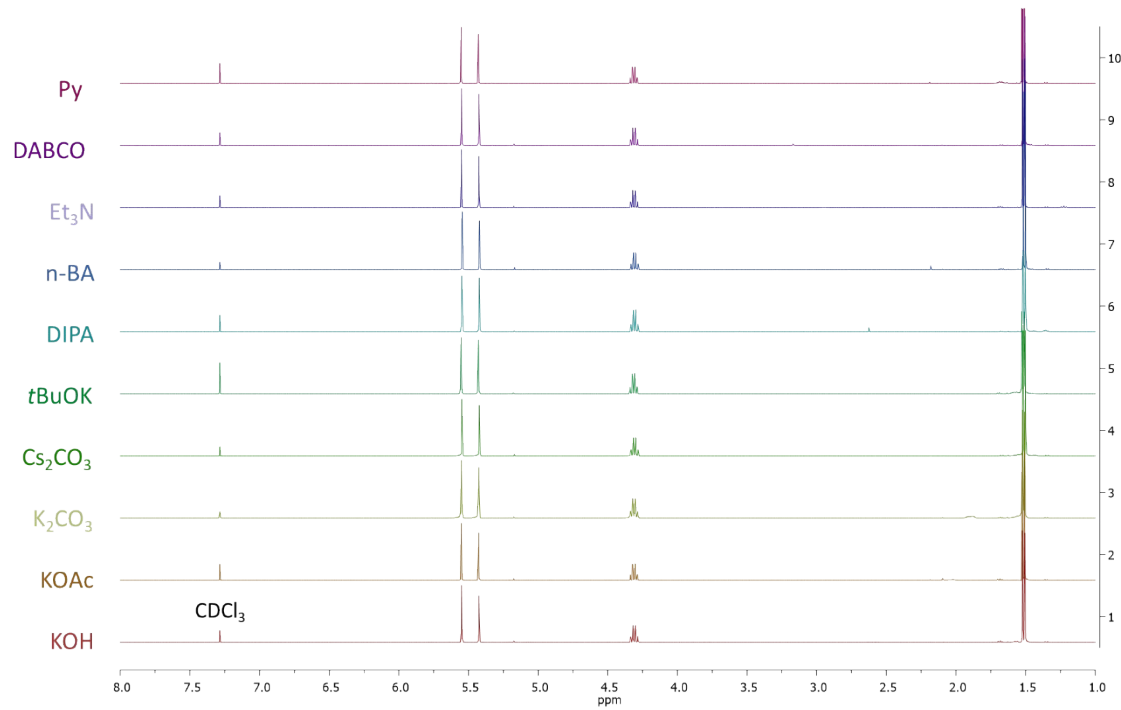


Fig. S21 ^1H NMR of LA-H,H (0.5mL) treated with different bases (0.07 mmol) at 100 °C for 24 h.

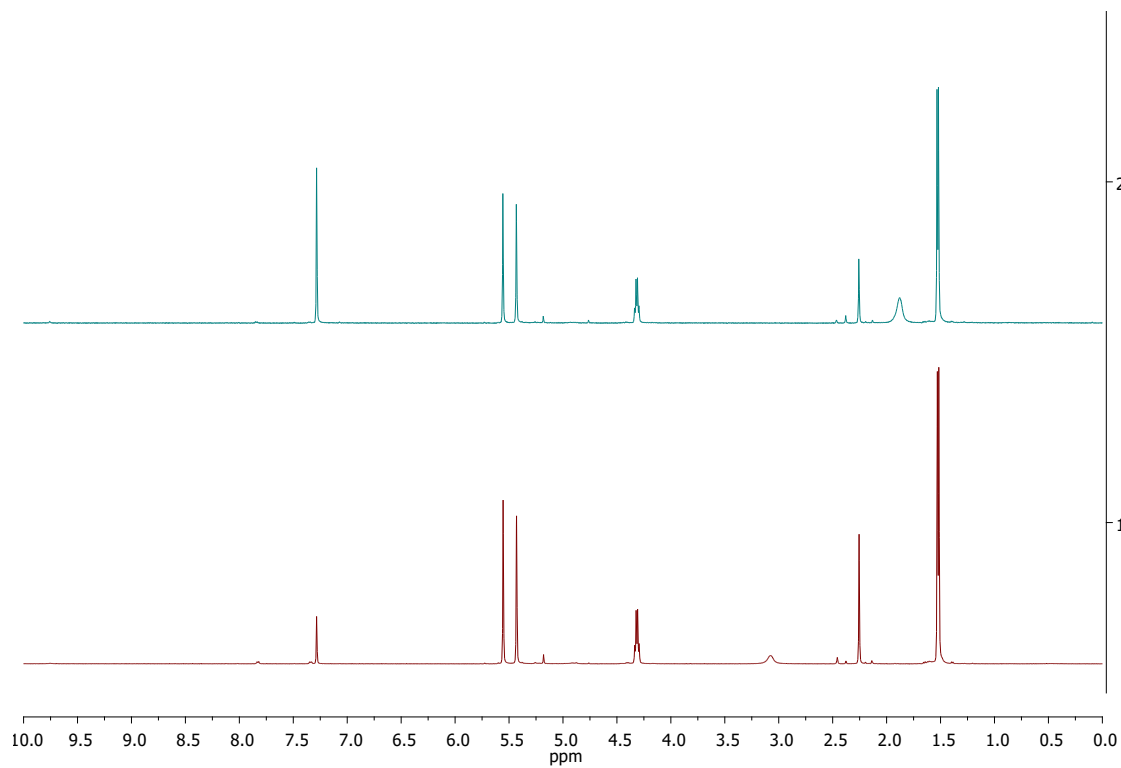


Fig. S22. ^1H NMR of LA-H₂H (0.5 mL) treated with *p*-TsOH for 24 h at RT (trace 1) and 50 °C (trace 2). HMB added as standard.

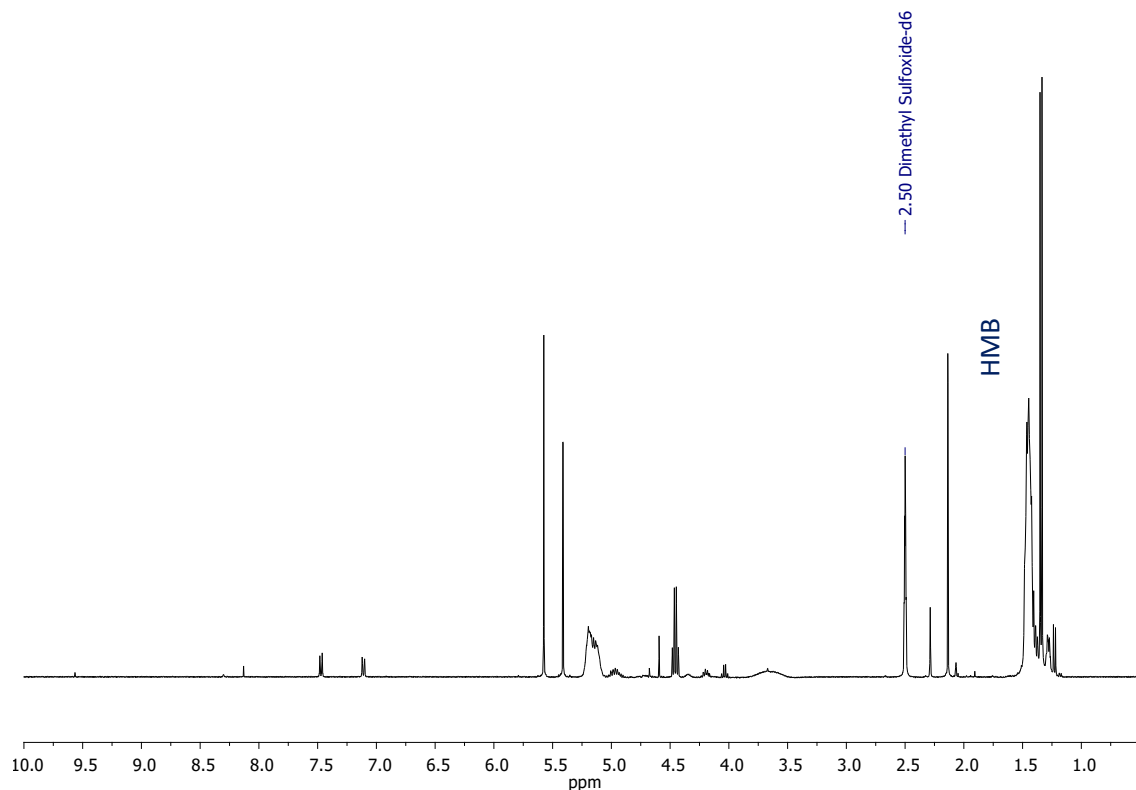


Fig. S23 ^1H NMR of LA-H₂H (0.5 mL) treated with *p*-TsOH (0.07 mmol) for 24 h at 100 °C. HMB added as standard.

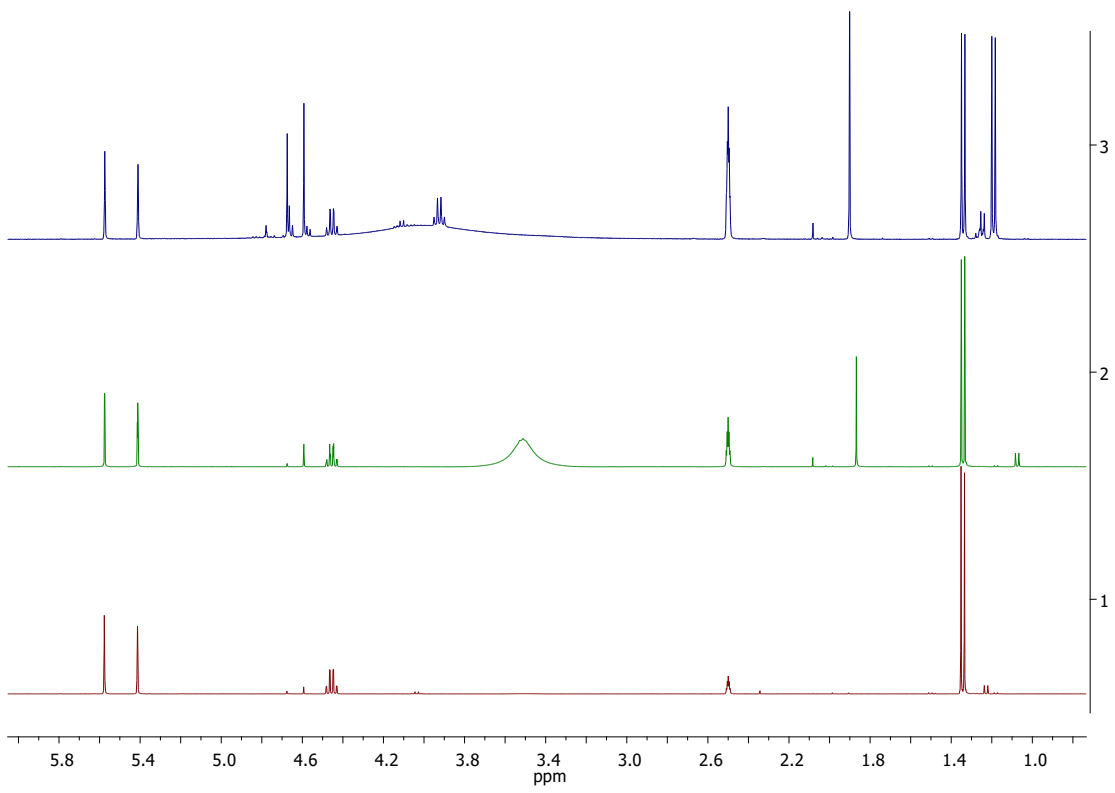


Fig. S24 ^1H NMR in DMSO-d₆ of LA-H₂H (0.5 mL) treated with concentrated HCl (5 μL, 0.07 mmol) for 24 h at RT (trace 1); 0.5 mL of acetic acid/sodium acetate buffer solution (pH 4.7) after 24 h (trace 2) and after two weeks (trace 3).

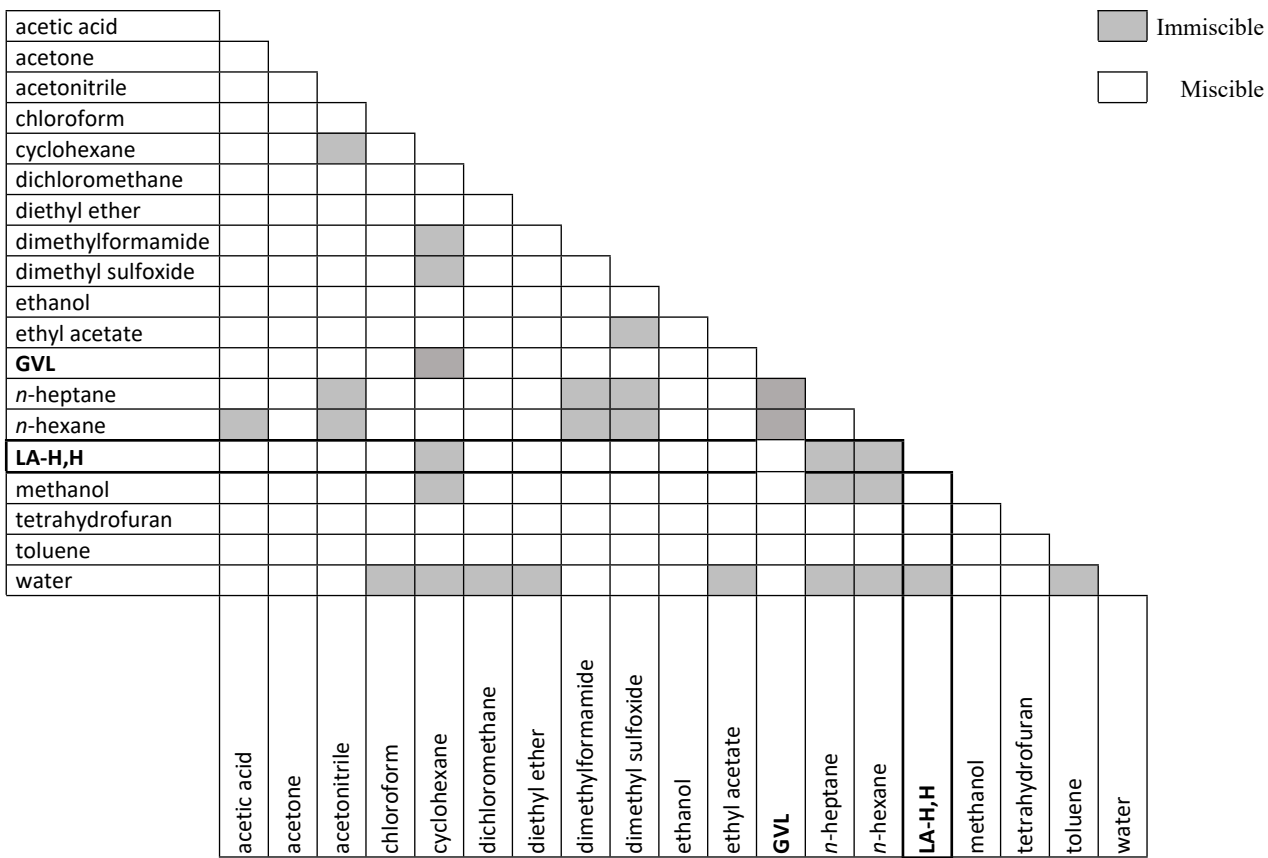


Fig. S25 LA-H,H miscibility table. Also LA-H,Me and MA-H,H resulted immiscible with *n*-hexane, *n*-heptane and cyclohexane., LA-Me,Me, iBu-H,H and iBu-Me,Me resulted miscible with *n*-hexane.

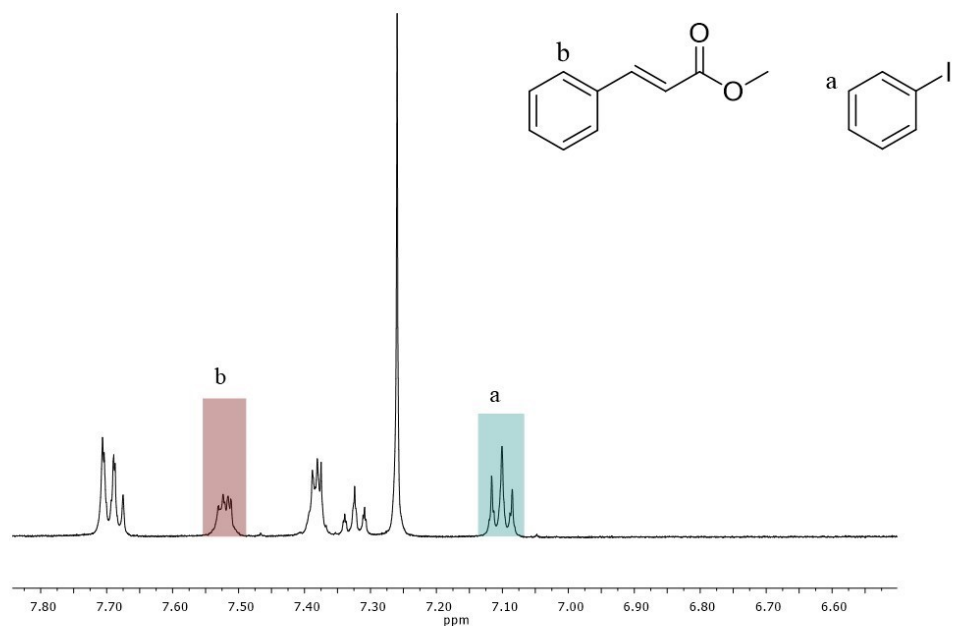


Fig. S26. Relevant portion of ^1H NMR of reaction mixture in presence of unreacted reagent (phenyl iodide) and product (methyl cinnamate). Yield is calculated by the following equation (13).

$$(13) \quad Yield (\%) = \left(\frac{\int_b}{\int_a + \int_b} \right) \times 100$$

Table S12 Mutagenicity and carcinogenicity *in silico* results. Average result: mutagenic – average score > 0.5; non-mutagenic average score <0.5; n.a. - not applicable.

Solvent	Software	Endpoint	Model	Results	Reliability	Score
LA-H,H	VEGA	Mutagenicity	CAESAR	Mutagenic	Low	0.5
			SARpy	Non-mutagenic	High	0.1
			ISS	Non-mutagenic	Moderate	0.3
			KNN	Mutagenic	Moderate	0.7
	TEST	Mutagenicity	Consensus	Non mutagenic	n.a.	0.12
		Mutagenicity	ISS	No alerts for <i>S. typhimurium</i> mutagenicity	n.a.	n.a.
	Toxtree	Carcinogenicity and mutagenicity	ISS	Negative for genotoxic carcinogenicity and for nongenotoxic carcinogenicity	n.a.	n.a.
			Average	Non-mutagenic	-	0.34
	VEGA	Mutagenicity	CAESAR	Mutagenic	0.7	
			SARpy	Non-mutagenic	0.3	
			ISS	Non-mutagenic	0.5	
			KNN	Non-mutagenic	0.3	
iBu-H,H	TEST	Mutagenicity	Consensus	Non-mutagenic		0.08
		Mutagenicity	ISS	No alerts for <i>S. typhimurium</i> mutagenicity	n.a.	n.a.
	Toxtree	Carcinogenicity and mutagenicity	ISS	Negative for genotoxic carcinogenicity and for nongenotoxic carcinogenicity	n.a.	n.a.
			Average	Non-mutagenic	-	0.37
	VEGA	Mutagenicity	CAESAR	Mutagenic	Low	0.5
			SARpy	Non-mutagenic	Moderate	0.3
			ISS	Non-mutagenic	High	0.1
			KNN	Non-mutagenic	Moderate	0.3
	TEST	Mutagenicity	Consensus	Non-mutagenic	n.a.	0.1
		Mutagenicity	ISS	No alerts for <i>S. typhimurium</i> mutagenicity	n.a.	n.a.
	Toxtree	Carcinogenicity and mutagenicity	ISS	Negative for genotoxic carcinogenicity and for nongenotoxic carcinogenicity	n.a.	n.a.
			Average	Non-mutagenic	-	0.27
MA-H,H	VEGA	Mutagenicity	CAESAR	Mutagenic	Low	0.5
			SARpy	Non-mutagenic	High	0.1
			ISS	Non-mutagenic	Low	0.5
			KNN	Mutagenic	moderate	0.7
	TEST	Mutagenicity	Consensus	Non-mutagenic	n.a.	0.13
		Mutagenicity	ISS	No alerts for <i>S. typhimurium</i> mutagenicity	n.a.	n.a.
	Toxtree	Carcinogenicity and mutagenicity	ISS	Negative for genotoxic carcinogenicity and for nongenotoxic carcinogenicity	n.a.	n.a.
			Average	Non-mutagenic	-	0.38
	VEGA	Mutagenicity	CAESAR	Mutagenic	Moderate	0.7
			SARpy	Non-mutagenic	Moderate	0.3
			ISS	Non-mutagenic	Low	0.5
			KNN	Mutagenic	Moderate	0.7
LA-H,Me	TEST	Mutagenicity	Consensus	Non-mutagenic	n.a.	0.08
		Mutagenicity	ISS	No alerts for <i>S. typhimurium</i> mutagenicity	n.a.	n.a.
	Toxtree	Carcinogenicity and mutagenicity	ISS	Negative for genotoxic carcinogenicity and for nongenotoxic carcinogenicity	n.a.	n.a.
			Average	Non-mutagenic	-	0.45
	VEGA	Mutagenicity	CAESAR	Mutagenic	Low	0.5
			SARpy	Non-mutagenic	Moderate	0.3
			ISS	Non-mutagenic	Low	0.5
			KNN	Mutagenic	Moderate	0.7
	TEST	Mutagenicity	Consensus	Non-mutagenic	n.a.	0.0
		Mutagenicity	ISS	No alerts for <i>S. typhimurium</i> mutagenicity	n.a.	n.a.
	Toxtree	Carcinogenicity and mutagenicity	ISS	Negative for genotoxic carcinogenicity and for nongenotoxic carcinogenicity	n.a.	n.a.
			Average	Non-mutagenic	-	0.40
iBu-Me,Me	VEGA	Mutagenicity	CAESAR	Mutagenic	Low	0.5
			SARpy	Non-mutagenic	Moderate	0.3
			ISS	Non-mutagenic	Low	0.5
			KNN	Mutagenic	Moderate	0.7
	TEST	Mutagenicity	Consensus	Non-mutagenic	n.a.	0.0
		Mutagenicity	ISS	No alerts for <i>S. typhimurium</i> mutagenicity	n.a.	n.a.
	Toxtree	Carcinogenicity and mutagenicity	ISS	Negative for genotoxic carcinogenicity and for nongenotoxic carcinogenicity	n.a.	n.a.
			Average	Non-mutagenic	-	0.40

Bibliography

1. US Environmental Protection Agency T.E.S.T. (Toxicity Estimation Software Tool) Version 5.1.2.0, [<http://www.epa.gov/ORD/NRMRL/std/cppb/qsar/index.html>].
2. Laboratory of Environmental Chemistry and Toxicology - Milan (Italy) - V.E.G.A. Version 1.1.5., [Italy<http://vegahub.eu/download/-vega-qsar-download/>].
3. G. Patlewicz, N. Jeliazkova, R. J. Safford, A. P. Worth and B. Aleksiev, *SAR and QSAR in environmental research*, 2008, **19**, 495-524.
4. S. A. Cairns, A. Schultheiss and M. P. Shaver, *Polymer Chemistry*, 2017, **8**, 2990-2996.
5. M. Okada, H. Sumitomo and M. Atsumi, *Macromolecules*, 1984, **17**, 1840-1843.
6. T. Miyagawa, F. Sanda and T. Endo, *Journal of Polymer Science Part A: Polymer Chemistry*, 2000, **38**, 1861-1865.
7. Y. Xu, M. R. Perry, S. A. Cairns and M. P. Shaver, *Polymer Chemistry*, 2019, **10**, 3048-3054.
8. D. L. J. Clive, W. Yang, A. C. MacDonald, Z. Wang and M. Cantin, *The Journal of Organic Chemistry*, 2001, **66**, 1966-1983.
9. K. Watanabe, Y. Andou, Y. Shirai and H. Nishida, *Chemistry Letters*, 2013, **42**, 159-161.
10. M. J. Kamlet and R. W. Taft, *Journal of the American Chemical Society*, 1976, **98**, 377-383.
11. D. J. Eyckens, B. Demir, T. R. Walsh, T. Welton and L. C. Henderson, *Physical Chemistry Chemical Physics*, 2016, **18**, 13153-13157.
12. M. J. Kamlet, J. L. Abboud and R. W. Taft, *Journal of the American Chemical Society*, 1977, **99**, 6027-6038.
13. H. L. Parker, J. Sherwood, A. J. Hunt and J. H. Clark, *ACS Sustainable Chemistry & Engineering*, 2014, **2**, 1739-1742.
14. Y. Marcus, *Journal of Solution Chemistry*, 1991, **20**, 929-944.
15. E. Stefanis and C. Panayiotou, *International Journal of Thermophysics*, 2008, **29**, 568-585.
16. M. Díaz de los Ríos and E. Hernández Ramos, *SN Applied Sciences*, 2020, **2**, 676.
17. C. M. Hansen and A. Björkman, 1998, **52**, 335-344.
18. F. Z. Jaime Lara, Daniel Drolet, Charles M. Hansen, Alain Chollet, Nathalie Monta, *International Journal of Current Research*, 2017, **9**, 47860-47867.